

FOR OFFICIAL USE ONLY

JPRS L/10454

13 April 1982

USSR Report

PHYSICS AND MATHEMATICS

(FOUO 3/82)



FOREIGN BROADCAST INFORMATION SERVICE

FOR OFFICIAL USE ONLY

NOTE

JPRS publications contain information primarily from foreign newspapers, periodicals and books, but also from news agency transmissions and broadcasts. Materials from foreign-language sources are translated; those from English-language sources are transcribed or reprinted, with the original phrasing and other characteristics retained.

Headlines, editorial reports, and material enclosed in brackets [] are supplied by JPRS. Processing indicators such as [Text] or [Excerpt] in the first line of each item, or following the last line of a brief, indicate how the original information was processed. Where no processing indicator is given, the information was summarized or extracted.

Unfamiliar names rendered phonetically or transliterated are enclosed in parentheses. Words or names preceded by a question mark and enclosed in parentheses were not clear in the original but have been supplied as appropriate in context. Other unattributed parenthetical notes within the body of an item originate with the source. Times within items are as given by source.

The contents of this publication in no way represent the policies, views or attitudes of the U.S. Government.

COPYRIGHT LAWS AND REGULATIONS GOVERNING OWNERSHIP OF MATERIALS REPRODUCED HEREIN REQUIRE THAT DISSEMINATION OF THIS PUBLICATION BE RESTRICTED FOR OFFICIAL USE ONLY.

JPRS L/10454

13 April 1982

USSR REPORT
PHYSICS AND MATHEMATICS

(FOUO 3/82)

CONTENTS

HIGH PRESSURE PHYSICS

Present State of High-Pressure Physics 1

LASERS AND MASERS

Promising Designs and Pumping Methods for Powerful CO₂
Process Lasers (Survey) 15

Change in Relaxation Rate of Upper Laser Level With Prolonged
Operation of Cw Electron-Beam-Controlled CO₂ Process Laser.. 44

OPTICS AND SPECTROSCOPY

Holographic Measurements 48

Feasibility of Controlling Gain of Enthalpy-Stimulated
Light Scattering 52

Conversion of Optical Radiation Spatial Spectrum in Parametric
Processes 57

- a - [III - USSR - 21H S&T FOUO]

FOR OFFICIAL USE ONLY

HIGH PRESSURE PHYSICS

UDC 53.092

PRESENT STATE OF HIGH-PRESSURE PHYSICS

Moscow VESTNIK AKADEMII NAUK SSSR in Russian No 9, Sep 81 pp 52-65

[Article by S. M. Stishov, doctor of physical-mathematical sciences]

[Text] Having arisen at the end of the 18th Century and the beginning of the 19th Century, high-pressure physics as a fully defined field of scientific research was finally formulated in the first third of our century. An outstanding role in this was played by P. V. Bridgman. Evidently, it was he who first introduced the term "High-pressure physics" publishing a book with this title in 1931,* in which he stated the results of his experimental research.

But neither P. Bridgman nor anyone else defined what would later be understood by high-pressure physics. Clearly, that of R. Feynman must be considered one of the best; it says, in essence: high-pressure physics is everything that physicists do with the help of equipment for creating high pressures. Actually, pressure up to many millions of atmospheres does not change the properties of substances. One cannot point to a single effect or phenomenon observed at around 1 million atmospheres that could not be observed in some form at atmospheric pressure (this means, first of all, phase transitions, electronic transitions, metallization, etc.). Thus, in experimentally achieved ranges of pressures, there is an absence of effects that are unique for compressed matter. In this connection, the situation in high-pressure physics in some sense is opposite to the situation in low-temperature physics, where the unique effects of quantum degeneration, superfluidity, superconductivity, and so forth are observed. However, it would be incorrect not to note that in the presence of very high pressures exceeding hundreds and thousands of atmospheres, we will find unusual riches of physical phenomena, including full ionization of matter, nuclear disintegration and nuclear reaction, neutronization of matter, superconductivity, and superfluidity in proton and neutron systems** (unfortunately, all this is unachievable directly by experimental study and conclusions can be only on the basis of astrophysical data). Thus, experimental high-pressure physics is nothing other than the "plain" continuation of the physics of atmospheric pressure in a new dimension, where the possibilities for experimentation are substantially increased and where the volume of information is vastly growing.

* For Russian translation, see P. V. Bridgman, "Fizika vysokikh davleniy" [High-Pressure Physics], ONTI, 1935.

** See D. A. Kirzhnits. "Uspekhi fiz. nauk" [Advances in Physical Sciences], 1971, vol. 104, p. 489.

FOR OFFICIAL USE ONLY

A few words must be said about pressure as a physical parameter. First, let us stress that the numerical significance of pressure, however large, says nothing about its effect on matter. The degree of such effect, obviously, must be considered the ratio of the work of compression which is determined by the integral $\int PdV$ to the size of the thermodynamic potential of the system $P=0$. Thus, the effect of pressure on matter is closely related to the response of the system to the applied effect, in the given instance, to compressibility. Because of this, a pressure of a million atmospheres turns out to have much less effect on less compressible matter (such as iron, for example) than several thousand atmospheres on extremely compressible matter such as helium. Hence comes the rule: in research on any phenomena, select objects that possess the highest degree of compressibility, other conditions being equal. This provides the possibility for investigating a phenomenon over a broad range of densities under relatively low pressures, and this is significant for conducting precision measurements.

The need for achieving very high pressures usually arises in the solution of specific scientific or applied problems. However, it is obvious that it is these specific problems that stimulate development of the technology and methods for high-pressures. A vivid example is the many year history of attempts to synthesize diamonds, which was brilliantly accomplished in 1955. As the result, diamonds and borazon (cubic nitride of boron) were synthesized, and high-pressure equipment was created that permits achieving pressures of about 100,000 atm in combination with temperature of up to 2000°C and higher. In turn, the new technology quickly found application in physics, chemistry, and technology. Especially striking results were achieved in geophysics in research on olivine-spinel transformation and polymorphism of silica. These results lie at the base of modern understanding of the structure and composition of layers of the earth. It must be noted that the aspiration to solve the puzzle of the earth's core is obviously one of the powerful incentives that will determine the development of high-pressure technology in the near future (the pressure at the earth's center is around 4 million atm).

CREATION OF HIGH PRESSURES

As follows from the equation of state $\phi(P,V,T)=0$, to create increased pressure, it is necessary in a corresponding manner to change the volume or temperature of the substance. Both means are used in practice.

Thermal means for creating pressure are fully effective for gasses. Multistage designs for gas thermal compressors are well known for creating pressures up to 10,000 atm. Autoclave technology is also widely used in science and industry. However, the direct compression of a substance is the most convenient means for creating pressure. In this case, it is necessary to have a strong vessel, which has at least one movable wall. The simplest and most popular design for such a type is the cylinder-piston type (fig. 1a).

As can be seen in the figure, in realizing this method, a strong, often many-layered, full cylinder is supplied with a piston and a plug. The cylinder is filled with liquid or previously compressed gas, and the piston and plug are correspondingly compressed. Usually, the plug serves as the place for locating electrical leads, which permit introducing detectors of various sizes into the

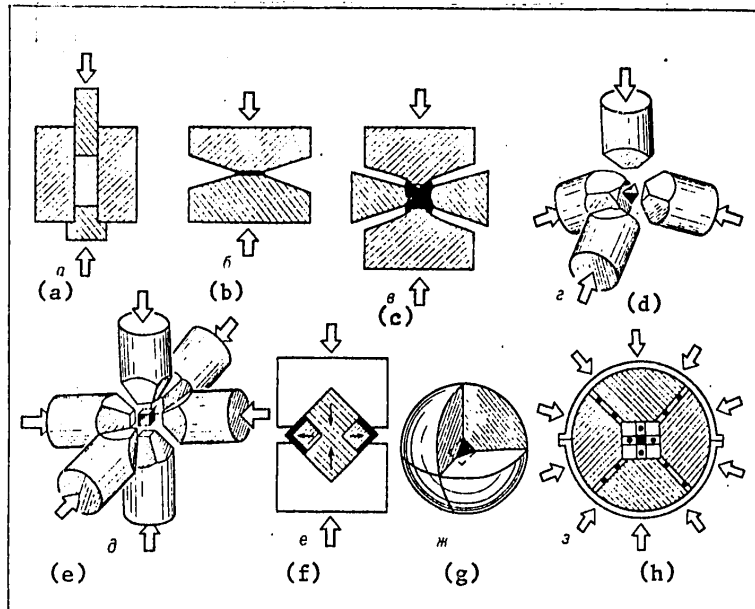


Figure 1. Sketches of High-Pressure Devices

- a. Cylinder-piston type chamber
- b. The Bridgman anvil (a thin layer of substance is compressed between two conic pistons)
- c. The "Belt" type device.
- d. The multiplunger tetrahedral device (four pistons located in the space along the diagonal of the tetrahedron simultaneously compress the specimen)
- e. Multiplunger cubic device
- f. Device with sliding anvils (limitations in the degree of compression are absent)
- g. Spherical multiplunger device; it differs from d and e in that the loading of the plungers is produced by loading the whole device in a high hydrostatic pressure chamber
- h. A two-stage spherical multiplunger device.

cylinder, first of all for temperature and pressure. To create pressure, the piston pushes down into the vessel with the aid of a screw or hydraulic press, but the limit in the pressure achieved in such a system is not at all determined by the power of the press, but the load-carrying capacity of the piston and cylinder. The strength of modern steel and hard alloys, in principle, permits using the cylinder-piston type system to achieve a pressure of 60,000 atm (the strength under pressure of the best instrument steel is about 350 kgf/mm², and hard alloys of the tungsten-carbide type cemented with cobalt, about 600 kgf/mm²). However, much before this, many problems arise with the sealing of

FOR OFFICIAL USE ONLY

compressed liquid or gas and, therefore, the field of hydrostatic pressure, that is, pressure that can be obtained by compressed gas or liquid, is limited to 30,000 or 40,000 atm.

In recent years, industry in a number of countries began to produce strong and flexible tubing of alloys with low heat conductivity having outside diameter of 1 to 3 mm and able to contain pressure of up to 20,000 to 25,000 atm. It became possible to separate spatially the pressure being created for the piston system and the vessel in which the research is being performed. This permits the creation of various specialized interchangeable chambers (optical, nonmagnetic, and others) and to locate them in a thermostat or cryostat, between magnetic poles, in an optical device, or a combination of these.

Using the piston system, it is possible to simplify the experiment and, in place of liquid or gas, to place inside the high-pressure chamber a plastic-solid body as the means of transferring pressure. Thus, the sealing problem is made simple, but complications arise in measurement and control of parameters, and nonhydrostatic components of stress appear. The pressure limits in such devices are 60,000 to 65,000 atm.

It turned out, however, that to achieve quasihydrostatic pressure (that is, achieved by compressing solids), other devices were more effective. Among them must be noted the Bridgman anvil, the "Belt" device, and multiplunger devices. The devices shown in Figure 1 b through h, with parts made of hard alloy, reach pressures of up to 200,000 atm, depending on design details. Recently, F. Bundy, of the General Electric laboratory, developed the "Belt" type of design, with a tip of synthetic polycrystalline diamond, capable of generating pressures of up to 500,000 atm.

All these devices can be adapted for conducting various physical, mineralogical, technological, and other experiments, including x-ray research on crystalline structure of matter.

In recent years, the diamond-anvil method has received widespread use (fig. 2). It began to develop intensively after the means was proposed for measuring pressure by the R-line shift of ruby luminescence (the wave length of ruby R-line luminescence is virtually linearly dependent on pressure).

The essence of the method is as follows. Two diamonds of jewel quality, polished in a special way (see fig. 2), are brought together by means of an uncomplicated lever-screw or hydraulic device. The specimen is placed directly between the working surfaces of the diamonds and, in this manner, a significant pressure gradient arises (see colored insert).^{*} Improved technology provides for placing the specimen together with a small piece of ruby in a washer made of strong and sufficiently plastic material, as shown in the insert (photograph 4). A hole in the washer is filled with a mixture of methyl and ethyl alcohol, which provides hydrostatic pressure up to 100,000 atm. At the present

^{*} Photographs were made by V. N. Kachinskiy, associate of the high-pressure sector of the Institute of Crystallography imeni A. V. Shubnikov of the USSR Academy of Sciences.

time, methods have been developed that permit using solidified inert gasses, including helium, as a means for transmitting pressure.

Characteristic dimensions of the device are as follows: diameter of the working surfaces, 0.3 to 1 mm; dimension of supporting surfaces, about 3 to 5 mm; the weight of each diamond, about 0.3 to 0.1 carat; the original thickness of the washer, 0.1 to 0.3 mm; and the diameter of the hole in the washer, 0.15 to 0.3 mm. The whole device will fit into the palm of a hand.

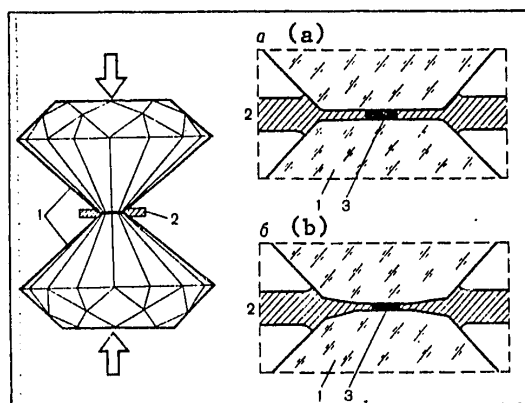


Figure 2. Diamond Anvils

1. Diamonds; 2. Metal washer; 3. Specimen;
 a and b are two types of diamond working surfaces:
 a -- simple anvils, and b -- with additional conic grinding of the working surface at a small angle, which reduces the stress gradient and permits the achievement of greater pressure.

With diamond anvils, it is possible to obtain extremely high pressures of up to 1.7 million atm.* The device is easy to use for conducting various optical, x-ray, Mossbauer, and other experiments. A virtue of this device of no little importance is the possibility of visual observation. **

In recent years, Academician L. F. Vereshchagin and his associates at the Institute of High-Pressure Physics of the USSR Academy of Sciences and, subsequently, A. Ruoff of Cornell University (United States) proposed using, to achieve very high pressures,

* See H. K. Mao and P. M. Bell. "Science," 1978, vol. 200, p. 1145.

** See S. Blok and D. P'yermarini [S. Block and D. Piermarini]. "Uspekhi fiz. nauk" [Advances in Physical Sciences], 1979, vol. 127, p 765.

5
 FOR OFFICIAL USE ONLY

FOR OFFICIAL USE ONLY

the indenter-plane type of device. It is clear that this device can develop very high contact pressures. However, this device can be used only to measure electrical resistance, and the value of this type of device for physical research is not very clear.

MEASUREMENT OF HIGH PRESSURES

There is a large number of instruments for measuring hydrostatic pressure. They include tubular, diaphragm, resistance, capacitance, and other manometers. However, all of them are secondary and need calibrating with calibration instruments. Such an instrument is the weighted piston manometer, in which an unknown pressure of a liquid is balanced with a weight, aided by the piston system. As a result, all that has to be known is the weight of the weight and the diameter of the piston. However, for precise determination of pressure, it is necessary to take into consideration the deformation of the piston and cylinder and the hydrodynamic effects arising in the flow of liquid through the gap, and so forth. Deformation corrections become especially large under pressures of 15,000 to 20,000 kgf/cm². The precision class of weighted-piston manometers in this range of pressures is no greater than 0.2 to 0.5. Thus, absolute accuracy of measuring pressure in this range cannot be less than 30 to 100 kgf/cm², and, consequently, the accuracy of pressure measurement by any secondary devices cannot be less than the magnitudes mentioned.

The most widely used secondary pressure sensor is the so-called manganin manometer, which is represented by a coil of manganin wire with resistance of about 100 ohms. The electrical resistance of the manganin rises almost linearly with pressure and possesses little temperature dependence at room temperature. In the use of the calibrating weighted piston manometer, secondary instruments can be calibrated up to pressures on the order of 30,000 to 35,000 atm without any substantial loss of accuracy and, consequently, it does not generate special problems in measuring pressure in this area. But under pressures exceeding these values, there are more than enough problems. The scale of pressures in this area is based on reference lines, for which phase transitions in certain elements and compounds are selected. The selection of reference substances is conducted with consideration for many factors, one of which is the ease of observation of phase transitions, for example, with the aid of measurement of electrical resistance. The pressures of phase transitions, which serve as reference points can be roughly determined with accuracy of the order of several kilobars with the aid of a cylinder-piston type of device within the limits of the pressure field, which does not exceed 60,000 to 70,000 atm. The determination of reference pressures lying outside this range have been based on extrapolations, rough assumptions, and often not even that much.

In 1965, D. Dekker proposed using as the basis of a scale for high pressures, an equation of state of the ion crystal NaCl and derived a corresponding semi-empirical equation suitable for calculating pressure with the aid of the results of measuring the density of NaCl under high pressures. And, although the precision of the proposed equation of state, evidently, was no higher than several percent (especially under high pressures exceeding 100,000 atm), the use throughout the world of NaCl as a standard nevertheless allows at least the production of comparable data.

At the present time, the pressures of reference lines are being redetermined on the basis of the NaCl scale. D. Piermarini, with coauthors from the U.S. National Bureau of Standards has calibrated the movement of the R-line of ruby under pressure through 300,000 atm on the NaCl scale. Subsequently, P. Bell and H. Mao

conducted calibration of a ruby sensor to 1 million atm, which was based on the equation of state of a number of metals that was determined with the aid of shock waves. These same authors lengthened the ruby scale to 1.7 million atm, having directly measured the contact area and distribution of pressure with various loads. The precision of the scale under such pressures is about 20 percent.

FUNDAMENTAL RESULTS OF RESEARCH UNDER HIGH PRESSURES

To explain the present situation in high-pressure physics and to evaluate its trends and prospects, it is necessary to analyze its results in some fashion. In the limited space of the present article, it clearly is not possible to try to describe the facts sufficiently and the more interesting projects, the more so because most of the achievements of high-pressure physics are fused together with the results of various subdivisions of physics, geophysics, crystal chemistry, and so forth. Instead of this, the author has undertaken the responsibility of trying to isolate and describe just those results that have had a deep influence on science and technology as a whole. There are undoubtedly such results and, in the opinion of the author, in first priority these must be the totality of phenomena discovered and described in the research of phase diagrams of matter, electronic phase transitions, the synthesis of diamonds and borazon, and geophysical research (phase diagram of silica). Let us look at these results in more detail.

Critical Point, Melting Curve

In 1869, T. Andrews, doing research on CO₂ condensation, discovered that beyond the temperature of 31° C, the condensation of gaseous CO₂ to a liquid takes place uninterrupted. The coordinates of the critical point for carbon dioxide Andrews determined to be 31° C and 76 atm. In his experiments, he used extremely modest experimental technology, and the pressures achieved did not exceed several hundred atmospheres. Let us stress that Andrews' discovery was the result of systematic research on equations of state and the condensation of gasses. The culmination of this research was the liquefaction of helium in 1908. Within three years after Andrews' discovery, J. D. Van-der-Waals formulated the theory that successfully described for the first time the critical phenomena in simple liquids.

The research of Andrews and Van-der-Waals provided a foundation for a number of areas in the physics of the condensed state of matter, the most important of which was the physics of phase transition and the physics of dense gasses and liquids.

The development of Van-der-Waals' ideas, the significance of which is stressed in every modern survey of phase transition, led to the creation of the integral equation method in the theory of liquids (the Born-Green-Bogolyubov-Kirkwood equation) and the later method of molecular dynamics, realized with the aid of large computers.

We must also note the recently developing research on critical phenomena in metals, where a nontrivial situation arises, since in this case, phase transition of liquid to steam is accompanied by the transition of metal to dielectric. This problem was first formulated by L. D. Landau and Ya. B. Zel'dovich. One of the first experimental projects in this field was done by I. K. Kikoin and A. P.

7
FOR OFFICIAL USE ONLY

FOR OFFICIAL USE ONLY

Senchenkov in 1967. Their research was closely related to the general problem of the metal-dielectric transition, which is also developing intensively at the present time.

The discovery of the critical point on the boiling curve became, in its time, a stimulating factor for the beginning of research on the melting curve. It was thought that it must end at a critical point, like the boiling curve. Much effort was spent in searching for the critical point on the melting curve by F. Simon, who did research on the melting curve of helium under high temperatures corresponding to a pressure of about 10,000 atm. But even under these pressures, the critical point was not discovered (it is interesting to note that not long ago (M. Besson) of Paris University traced the melting curve to the temperature of 25° C and pressures of around 115,000, with the aid of the technology of diamond anvils.

A large number of such experiments were conducted by P. Bridgman, who was extremely skeptical about the possibility of the existence of the critical point on the melting curve. However, from the theoretical point of view, the situation was unclear until L. D. Landau in 1937 showed the impossibility of the existence of a critical point on the melting curve.

A wide discussion arose at one time on the question of the form of the melting curve. P. Bridgman insisted that with the growth in pressure, the increase in the temperature of a melting substance is unlimited. G. Tamman asserted that the temperature of the melting of any substance must pass through a maximum. As we now know, there is no general solution to this problem. The answer depends on the form of interparticle interaction and the role of quantum effects in a given system of particles. Let us stress that the capability for melting-crystallization is a fundamental property of multiparticle systems, independent of their specific nature. Therefore, one must think that the phenomena of melting-crystallization play an important role in the evolution of white dwarfs, pulsars, and other astronomical objects.

Electronic Phase Transitions

Insofar as reduction of interatomic distances lead to expansion of bands of electronic states and to the reduction of energy distances between them, it can be expected, from very general considerations, that increase in pressure will stimulate the occurrence of phase transitions due to transitions of electrons from band to band (including transitions of the metal-dielectric type). This also takes place in reality. Transitions of such a type can be seen as a precursor of phenomena that under further increase in pressure finally lead to the disappearance of the shell structure of the atom generally.

A remarkable example of a transformation of such a type is the phase transition in cerium found first by P. Bridgman, with pressure of about 7,000 atm and at room temperature; in connection with this, the density of cerium increases by 15 percent. Since, under atmospheric pressure, cerium already possesses a close-packed structure, L. Pauling and V. Zacharias proposed that in cerium there is a transition of an electron from band 4 f to 5 d.

A. Lawson and T. Tang with x-ray structural analysis demonstrated that phase transition in cerium is isostructural, that is, it does not change the symmetry or

the type of packing. In 1958, Ye. G. Ponyatovskiy revealed that with increased temperature, the heat of the phase transition in cerium approaches zero along the line of the phase transition and proposed that the phase transition curve in cerium would end at a critical point. Subsequently, Ye. G. Ponyatovskiy's results were fully confirmed.

Let us stress that the critical point in cerium is completely analogous to the critical point of the liquid-vapor type (the symmetry of cerium does not change with phase transition). It would be interesting to know the significance of critical indices at this point (one should think that, in this instance, it would be possible to observe the applicability of an average field theory).

A critical point is expected also on the curve of isostructural phase transition in SmS, which is simultaneously a metal-dielectric transition. Let us note that phase transitions of the metal-dielectric type in chalcogenides of rare-earth elements at the present time are a subject of numerous research projects, including applied ones.

An extremely interesting phase transition that is evidently tied with electron transition from a 6s- to a 5d-state takes place in cesium under pressure of about 40,000 atm. This transition was also discovered by P. Bridgman, but J. Bardeen suggested its electronic nature. Calculations by R. Sternheimer confirmed these proposals. Decisive results were achieved by T. Hall and his coworkers which, using x-ray analysis, showed that phase transition in cesium is isostructural. Unfortunately, because of technical difficulties, this transition has been studied in less detail than the transition in Ce and SmS. It must be pointed out that in the case of electronic transitions, the real situation evidently cannot be described by simple diagrams of transitions between two electronic states. At least, recent experiments in Compton scattering do not support the diagram proposed by L. Pauling and V. Zacharias for the transition in Ce.

If, as a result of change in the energy state of electrons, there is a disappearance of the energy gap dividing the band of valence electrons and the conduction band the substance acquires metallic properties. Such transitions are called metallization or metal-dielectric transitions. Evidently, metal-dielectric transitions were observed for the first time by P. Bridgman, doing research on electrical resistance in tellurium and black phosphorus. Later, in the 1960's, a series of projects on metal-dielectric transition has been conducted by H. Drickamer and associates.

At the present time, a large number of elements and compounds are known that have transitions into metallic states under pressure; these are tellurium, selenium, sulfur, iodine, germanium, silicon, and a number of compounds of types $A^{III}B^V$ and $A^{II}B^{VI}$ and others. Some of these substances are being found to have superconducting properties in the metallic state.

Metallization can take place as a clearly expressed phase transition of the first kind with sharp change in crystal structure and electrical properties as, for example, in Ge, Si, and other substances with coordination structure. In other cases, especially in substances of the molecular type, such as S and Se, change in electrical properties takes place gradually within the range of several tens or even hundreds of kilobars.

9
FOR OFFICIAL USE ONLY

FOR OFFICIAL USE ONLY

It must be noted that a sharp and reversible metal-dielectric transition in amorphous germanium, silicon, and indium antimonide was recently observed under high pressures by S. Minomura and associates at Tokyo University.

Synthesis of Diamonds and Cubic Nitride of Boron

In 1955, the research laboratory of the General Electric firm announced success in the synthesis of diamonds, and in 1959 a Detroit factory of the firm began series product manufacture.

Having gone into the "diamond" research group, T. Hall invented the "Belt" high-pressure device, which helped bring about the first diamond synthesis, and also a series of multiplunger devices. Soon, R. Wentorf synthesized borazon. Subsequently it turned out that Swedish researchers had produced artificial diamonds before the Americans, but had kept their results secret. In the USSR, the first synthetic diamonds were produced at the Institute of High-Pressure Physics of the USSR Academy of Sciences under the direction of Academician L. F. Vereshchagin. Let us stress that success was achieved as the result of using new conceptions in the design of devices and application of catalysts (metals of the transition group).

At the present time, the diamond industry has been developed in many countries around the world and, evidently, provides industry with material suitable for manufacturing grinding wheels, diamond paste, and so forth. However, the need for large diamonds for manufacturing cutting tools, draw plates, drilling tools, and so forth, continues to grow. It is satisfied by natural diamonds and also by baked synthetic material (General Electric compact) and synthetic material of the carbonado type manufactured in the USSR.

At the beginning of the 1970's, a research group at General Electric again met with success in growing monocrystals of jewel quality diamonds 5 to 6 mm in size. However, the process of growing jewel-grade diamonds is still too expensive for industrial production. Nevertheless, it must be expected that it will be improved and that in the end, industry and science will be furnished this material in sufficient quantities. Much still must be done in this area, particularly in understanding fully the mechanism of catalytic action in diamond synthesis and the natural mechanism of diamond formation. It is possible that a way will be found to lower the parameters of diamond synthesis. It is no less important to manufacture larger components from polycrystal diamond. This undoubtedly will have a revolutionary effect on the technology of high pressures. The first attempts in this area are very hopeful.

Geophysical Research

The study of the internal structure of the earth and other planets is extremely fascinating and has practical importance, but is still an unsolved problem. The first conceptions, which pictured the earth as a kind of gigantic metallurgical furnace with its composition divided into slag, matte, and metal, rather soon ceased to satisfy researchers. The accumulation of data on the thermodynamic and mechanical properties of the internal layers of the earth led to the conclusion that the presence of significant quantities of heavy metals and their sulfides in the earth's mantle (that is, to a depth of about 2900 km) is not possible. An analysis

conducted by the American geophysicist F. Burch in 1952 showed that the material composing the lower mantle must possess a very high ratio of the bulk modulus to density -- $k/\rho \approx 60 \text{ (km/s)}^2$; this is typical for oxides of the MgO and Al_2O_3 type, but is not possible for silicates that compose the surface layers of the earth. F. Burch suggested a hypothesis about the possibility of the existence in the depths of the earth of new polymorphic modifications of silicates, which would contain silicon in sixfold coordination relative to oxygen (instead of the usual fourfold). This hypothesis later suffered criticism, the more so because the first attempts at experimental verification did not lead to positive results. However, in 1961, the present author and S. V. Popova achieved a new dense modification of silica under pressure of about 100,000 atm and temperature of 1500°C . The crystalline structure of this modification is equivalent to the crystalline structure of rutile (TiO_2) and contains silicon in sixfold coordination relative to oxygen. The density of the new modification of silica turned out to be 4.35 g/cm^3 , or 64 percent more than the density of quartz.

Thus, the hypothesis of the possibility for significant compression of silicates under the action of pressure was proved. Later this permitted constructing a model of the lower earth mantle, which successfully explained the data of observations without drawing upon concepts about changes in the chemical composition of the mantle with depth. It is interesting that subsequently rutile-like silica was discovered in nature. This modification was found for the first time in an Arizona meteorite crater by associates of the U. S. National Geological Service headed by E. Chao.* At the present time, the finding of this unusual mineral, and also another dense modification of silica, (coesite), produced by (L. Coes) in 1953, is evidence of the impact origin of a number of geological structures.

The significance of high-pressure physics is not exhausted by the striking results, some of which have been described above. Actually, when the investigation of a phenomenon requires variation in the density of a substance under constant temperature or, in reverse, variation in temperature with constant density, the methods of high-pressure physics are used. Therefore, the influence of the methodological achievements of high-pressure physics on the development of knowledge perhaps exceeds the influence of its "own" results.

THE PRESENT STAGE IN THE DEVELOPMENT OF HIGH-PRESSURE PHYSICS

The present situation in high-pressure physics to a significant degree is determined by the peculiar history of its development. The point is that research in this area of physics was not too popular in the first half of the present century because of the great methodological difficulties. However, in the 1950's, the situation changed abruptly. In announcing the synthesis of diamonds, researchers at General Electric gave a powerful impetus to the development of the technology of high pressures and inspired many scientists to search for new phases with properties perhaps even more notable than diamonds and borazon. Thus, a new industrial period in high-pressure physics was initiated.

Looking back, one can say that the hopes for creating new materials with astonishing properties, generally speaking, have not materialized. And, although the scientific results of research under high pressures have been significant (especially geophysical problems must be singled out), nothing comparable with diamond synthesis

* The new material was named "stishovite" in honor of S. M. Stishov, the author of the present article. -- Ed.

FOR OFFICIAL USE ONLY

has been done. A wave of a kind of disillusionment ensued. But, by the end of the 1960's and beginning of the 1970's, a new enthusiasm began. One of the reasons was the development of the diamond anvils described above, which allowed the production of a very high pressure. Another reason for the noticeable revival of experimental and theoretical activity in the field of high-pressure physics was related to the hope of producing metallic hydrogen. However, in the opinion of the author, the present period of upsurge still seems to be an echo of the "diamond" boom in the sense that at its base, possibly, lies a lack of good ideas among a surplus of professionals.

The idea of transforming molecular hydrogen into a metallic state under high pressure was suggested many years ago in connection with the discussion of the internal structure of the planets Jupiter and Saturn. In 1935, E. Wigner and (H. Huntington) conducted the first calculations and evaluated the pressure for the transition of hydrogen to a metallic state. A more precise and complete calculation was conducted by A. A. Abrikosov in 1954. Later, V. P. Trubitsyn was engaged in this problem. However, the hydrogen problem did not attract special attention until, in 1968, N. W. Ashcroft produced results that indicated possible metastability of hydrogen under atmospheric pressure and the potentially high temperature (~100 K) of superconductive transition to metallic hydrogen.

Soon after this, (Ye. G. Brovman) and Yu. M. Kagan showed that the hypothetical metastable metallic hydrogen can have an extremely unusual filamentary structure, representing a kind of hybrid liquid and crystal.

All this caused unprecedented enthusiasm among a wide scientific community. Some experimental groups announced their plans to produce metallic hydrogen.* Let us stress that, according to various evaluations, the pressure for transition of hydrogen to a metallic state is a magnitude of about 2 million atm. If one takes into consideration that, from the beginning of the "hydrogen" boom, no one in the world has achieved a static pressure even approaching this limit,** one must only be surprised at the boldness of the authors of various projects.. Relative to this, one can recall the words of Nobel laureate A. A. Szent-Gyorgyi. Going fishing with a large hook, he said: "I know I won't catch anything anyway, but it's more pleasant not to catch a big fish than a little one."

In any case, work began. At first, it seemed that success might be achieved by using large multiplunger systems or multistage devices. The group of A. Ruoff of Cornell University built for this purpose a spherical six-plunger device (see fig. 1 h) with a diameter of over a half meter. A group at the Institute of High-Pressure Physics of the USSR Academy of Sciences intended to use for obtaining metallic hydrogen, a gigantic press with 50,000 tons of force; however, it did not report any details about a chamber in which a pressure of millions of atmospheres could be produced.

It must be stated that physicists who plan experiments with hydrogen at one time underestimated miniature and modest devices such as the diamond anvil. Meanwhile,

* For more detail, see S. M. Stishov. "Uspekhi fiz. nauk" [Advances in Physical Sciences], 1979, vol. 127, p. 721.

** We ignore without comment any statements about achieving superhigh pressures that are not accompanied by proofs at even a common-sense level.

geophysicists and geochemists, engaged in a literal sense with earthly cares, saw in diamond anvils a means for modeling P-T conditions corresponding to those of the lower earth mantle. Geophysical research applying diamond anvils began to develop rapidly. One of the most important results achieved in this field of research must obviously be considered the establishment of the fact that magnesia pyroxene ($MgSiO_3$) under pressures of around 250,000 atm acquires the structure of the pyroxite type, extremely effective from the point of view of packing. The fact that, in crystalline structures of this type, large cations (in this case, magnesium) are included in very dense packing formed by anions. Record results were achieved in the geophysical laboratories of the Carnegie Institute (United States), where P. Bell and H. Mao were successful, with the help of diffractions of x-ray beams, in studying equations of state of geophysically interesting materials, MgO and Fe, up to 1 million atm. These same authors, as noted above, reported on the achievement of pressures of about 1.7 million atm in diamond anvils. Having such technology available, it was difficult to ignore the temptation to do research on hydrogen. In 1979, P. Bell, H. Mao, and S. K. Sharma compressed hydrogen up to ~650,000 atm and investigated its Raman spectra. The results of this work show that the frequency of intramolecular oscillation in hydrogen begins to decrease under pressures exceeding 300,000 to 350,000 atm. This is undoubtedly evidence of approaching the instability of the molecular phase of hydrogen. Without examining the results of dynamic experiments, the integration of which cannot be conducted directly, it must be asserted that research on the Raman spectra of hydrogen under pressures of up to 650,000 atm is practically the whole of the "dry bones" of ten years of controversy and discussion of plans and, to a far lesser degree, real experimental projects.

The information that occurs in the literature that, under static compression of hydrogen equal to that of other substances, a sharp drop in electrical resistance is observed, apparently must be accepted with caution. Actually, A. Ruoff's results in measuring electrical resistance of xenon, which seem to be a clear indication of its metallization under pressure of about 300,000 atm, have turned out to be incorrect, despite the special measures undertaken by the author to avert the short-circuiting of the electrodes.

It must be expected that research on hydrogen under high pressure in the present decade will be continued, in view of the undoubted physical interest in the problem. Clearly, it must have a more systematic character and develop on the whole plane of research in compressed gasses under superhigh pressures. Already, now, in the Carnegie Institute geophysical laboratory, at Los Alamos Laboratory, the University of Paris, and Paderborn University (FRG), optical and structural research is being conducted on nitrogen, oxygen, xenon, and helium with diamond anvils. Undoubted interest is presented also by the study of the possibility for producing metallic ammonia,* the field of stability of which nearly coincides with the field of stability of metallic hydrogen.

Despite lack of success in achieving the direct goal of producing metallic hydrogen, the "hydrogen" problem as a whole has had a strong influence on the psychology of experimentors. It has become clear that, first of all, the advance toward higher pressures is not possible without using natural or synthetic diamonds and, secondly, gigantic presses and devices must, at least temporarily, yield to miniature devices of the diamond anvil type.

* See S. M. Stishov. "Uspekhi fiz. nauk" [Advances in Physical Sciences], 1978 vol. 125, p. 731.

FOR OFFICIAL USE ONLY

The realization of these truths has led to the wide distribution of diamond anvils and to the development throughout the world of optical and x-ray research under high pressures. Pressure limits achieved in laboratories have increased from 150,000 to 200,000 to 1 million atm and more. It is notable that the development of the diamond anvil technology has coincided with the development of new, effective methods in optics and spectroscopy, x-ray radiography, and so forth, which combines well with the application of diamond anvils. At the present time, a number of laboratories use coordinate and semiconductor detectors for recording x-ray diffractions from the specimen placed in diamond anvils. The application of these means permits substantial decrease in exposure, compared with photographic methods, and improvement in the quality of the primary information. For example, the use of the linear coordinate detector in combination with diamond anvils allowed S. Minomura and his associates to explain for the first time the details of behavior of iodine under a metal-dielectric phase transition. It turned out that the gradual metallization of iodine while preserving the molecular-type crystalline structure is accomplished under pressures of about 200,000 atm with uneven transition to fully dissociated crystalline structure in which it is no longer possible to isolate individual I_2 molecules. The possibility is not excluded that this is the manner in which metallization of hydrogen will take place.

The application of a semiconductor detector of 30-mm diameter in the laboratory of (W. Holsapfel) at Paderborn University permits the production of x-ray diffraction spectrum of a powdered specimen located in diamond anvils for 2 to 3 minutes which provides the possibility of studying the kinetics of phase transitions.

It is apparent that in the next few years, research in high-pressure physics will be tied to diamond anvils. It must be expected that increase by almost one order of magnitude of the limits of achieved pressures will bring results. Unfortunately, this effective technology, for a number of reasons, has not been developed in the USSR. However, the situation has now changed. The Institute of Crystallography imeni A. V. Shubnikov of the USSR Academy of Sciences has developed various alternative devices with diamond anvils and has demonstrated the suitability of diamonds from Yakutsk deposits for achieving pressures on the order of a million atmospheres and the beginning of real experimental work. Appropriate projects have also been started in other USSR scientific institutions. One must not think, however, that diamond anvils will be successful in solving all the problems of high-pressure physics. The limited size of the specimen and insufficient precision for certain types of pressure measurement sometimes force the preference for the experimental technology of hydrostatic and quasi-hydrostatic pressures.

Unfortunately, standard equipment for high pressure is not manufactured in the USSR, and this substantially limits the application of high-pressure physics methods in experimental work.

Evaluating the situation as a whole, it must be stressed that high-pressure physics has entered a new, practically untouched range of pressures, and it is necessary to decide how to introduce its achievements most effectively into general experimental physics, geophysics, and other branches of knowledge.

COPYRIGHT: Izdatel'stvo "Nauka", "Vestnik Akademii nauk SSSR", 1981

9645

CSO: 8144/0466

FOR OFFI

LASERS AND MASERS

UDC 621.378.324

PROMISING DESIGNS AND PUMPING METHODS FOR POWERFUL CO₂ PROCESS LASERS (SURVEY)

Moscow KVANTOVAYA ELEKTRONIKA in Russian Vol 8, No 12(114), Dec 81 (manuscript received 24 Dec 80, after revision 23 Apr 81) pp 2517-2539

[Article by G. A. Abil'sitov, Ye. P. Velikhov, V. S. Golubev and F. V. Lebedev, Scientific Research Institute of Process Lasers, USSR Academy of Sciences, Troitsk, Moscow Oblast]

[Text] An analysis is made of the prospects for developing powerful CO₂ gas-discharge process lasers with respect to methods of cooling the working medium, possible gasdynamic and optical arrangements and pumping methods. An examination is made of physical and technical problems of using gas discharge in laser devices. The authors discuss the limiting and operational characteristics of various kinds of process lasers and the most advisable fields of application.

Contents

Introduction

1. Designs of CO₂ gas-discharge lasers
 - 1.1. CO₂ lasers with diffusion cooling of working mixture
 - 1.2. Fast-flow CO₂ gas-discharge lasers
2. Methods of pumping gas-discharge lasers
 - 2.1. Self-maintained dc discharge
 - 2.2. Semi-self-maintained discharge with electron-beam ionization
 - 2.3. Semi-self-maintained discharge with ionization by periodic pulses
 - 2.4. Ac discharge

Conclusion

Introduction

Research over the past decade on interaction of powerful laser radiation with matter has opened up new prospects for using lasers to process materials, and also demonstrated some fundamental advantages of laser technology over conventional forms of handling materials. Laser cutting and welding, heat-treatment, plating and alloying are not only productive and economically effective, but also can frequently be used to get items with characteristics unattainable by other technological methods.

15
FOR OFFICIAL USE ONLY

FOR OFFICIAL USE ONLY

Of particular interest for laser technology are powerful lasers (more than 1 kW), and first of all gas-discharge CO₂ lasers. This is because of their simplicity, high efficiency, and also the capability for getting high power and brightness of radiation in relatively compact laser facilities.

The working principle of the molecular CO₂ laser was formulated by Patel [Ref. 1] in 1964; the first laser that he produced with glow-discharge pumping [Ref. 2] had a power of 1 mW. However, within only a year the power of the CO₂ laser had reached 10 W at efficiency of 10%, and in 1967 it was 500 W with cw operation [Ref. 3].

A further appreciable increase in the power of CO₂ lasers became possible with the advent of convective cooling of the working mixture [Ref. 4]. The CO₂ laser developed in 1969 with transverse pumping of the lasing mixture had a power of ~1 kW [Ref. 5]. Use of a semi-self-maintained discharge kept alive by electron beam raised the power of fast-flow lasers to 15 kW as early as 1972 [Ref. 6].

At the present time there are a large number of different stationary systems with power of 1-15 kW. There have been reports on developing and using stationary lasers of open type with power from 20 to 100 kW in technological experiments [Ref. 7]. Nevertheless, most of the described laser systems are of the experimental laboratory type and are intended chiefly for clarifying and checking principles of construction of powerful lasers rather than for use in industry.

In addition to the necessary power, the industrial process laser must have a number of specific features. It must be distinguished by high stability of emission power, and meet the requirements for technological machine-building equipment: high reliability and economy, simplicity of design and ease of control, small overall dimensions and long service life, as well as guaranteeing high safety of servicing. Many nations of the world are now engaged in the development of powerful CO₂ laser devices for machining materials.

At the present time, several surveys have already been published that deal with the principles of CO₂ laser operation [Ref. 14, 15], problems of stability of gas discharge in molecular gases [Ref. 16-19], and also with the prospects for development of powerful gas lasers [Ref. 20, 21, 33]. However, as a rule they have not examined specific methods of excitation of the medium, or such questions of importance for practical application as simplicity of implementing these methods, efficiency of the laser as a whole, advantages and disadvantages of different gas-dynamic and electro-optical arrangements.

In this survey, in addition to the generally accepted classification of gas-discharge CO₂ lasers according to cooling methods, we give their classification by gasdynamic and electro-optical arrangements, working conditions of cavities, and methods of gas-discharge pumping, as well as examining the most advisable fields of application and the limiting characteristics of different laser systems. Particular attention is given to description and analysis of different gas-discharge arrangements used for excitation of the active medium of CO₂ lasers. Not only the physical, but also the technical aspects of implementing these arrangements are discussed.

FOR OFFICIAL USE ONLY

1. Designs of CO₂ gas-discharge lasers

In the CO₂ laser, stimulated emission takes place on the transition between vibrational energy levels 00⁰¹ and 10⁰⁰ of the CO₂ molecule [Ref. 1, 2]. The quantum efficiency of this transition, corresponding to emission of quanta with wavelength of 10.6 μm, is fairly high: $\eta_{KB} \approx 0.4$.

Due to heat release upon lasing of the mixture (5-10% of the energy released in the discharge goes to heating), and collisional relaxation of the upper laser level, the processes of pumping of the laser mixture and stimulated emission are unavoidably accompanied by heating of the gas, the temperature T_r of the lasing mixture in the steady state being practically proportional to the power of the energy release in the discharge.

In the absence of lasing, the population of the upper laser level is proportional to the intensity of energy release in the discharge, and consequently (disregarding dependence of the cross section of collisional relaxation σ_r on gas temperature), to the gas temperature as well. This relationship can only be weakened by accounting for the dependence of σ_r on T_r .

The population of the lower lasing level is determined by collisional processes, and at radiation intensities that are not too great it corresponds to Boltzmann law, i. e. it increases exponentially with increasing T_r . In this connection, upon attainment of a certain critical temperature $T_{kp} \sim 500-600^\circ\text{C}$ [Ref. 22], inverse population of the laser mixture disappears. The maximum inversion is attained at a mixture temperature of $T_{opt} \sim 200-300^\circ\text{C}$.

Thus, one of the principal conditions of CO₂ laser operation is inadmissibility of overheating the laser mixture beyond T_{opt} , i. e. availability of efficient cooling. At the present time, classification of electric-discharge lasers has been proposed in accordance with methods of cooling the laser mixture and stabilizing the discharge [Ref. 20, 21]. The sense of this classification is illustrated by Fig. 1.

In lasers of the first type (discharge tube coaxial with the optical system), the laser mixture is cooled and the discharge is stabilized by diffusion processes. The heat released is carried off to the cooled wall of the laser tube via molecular diffusion, and ambipolar plasma diffusion prevents discharge contraction. The presence of gas flow in lasers of this type is not in principle necessary, and its role is reduced to preventing poisoning of the active medium as a result of various plasma-chemical reactions [Ref. 23].

In lasers of the second type, differing from the first only in rapid circulation of gas through the discharge tube, discharge stabilization is handled as before by ambipolar diffusion; however, the temperature of the laser mixture is maintained on the admissible level by the rapid rate of gas circulation (convective cooling).

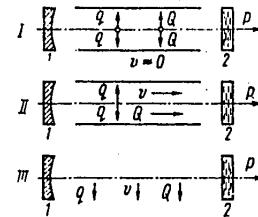


Fig. 1. Types of CO₂ lasers: v--gas flow velocity; Q--heat flux; q--charged particle flow, P--quantum flux; 1--opaque mirror; 2--output mirror

FOR OFFICIAL USE ONLY

Finally, in lasers of the third type the gas is circulated in the direction perpendicular to the optical axis. In this case, it is the rapid gas flow that prevents both overheating of the mixture and discharge transition to arcing.

It should be noted that such a classification does not always reflect the principle of discharge stabilization or particulars of the electro-optical arrangement of the laser. The characteristic diffusional dimension is not always determined by the radius of the glass tube or the size of the discharge zone. At high gas velocities, charge diffusion due to flow turbulence may exceed ambipolar diffusion and play an appreciable part in discharge stabilization. The discharge may be stabilized not only by diffusion, but also by electronic means (combined action of electric fields [Ref. 24], rotation of the electric field vector in space [Ref. 25], etc.). Flow in the direction perpendicular to the optical axis does not preclude diffusional discharge stabilization [Ref. 26]. Moreover, depending on the degree of flow turbulence, the same electric diagram of a laser may be classified as both type II and type III [Ref. 26]. Therefore, hereafter we will divide all lasers with respect to type of mixture cooling (diffusional, convective).

One of the most important characteristics of the laser is its efficiency. The total efficiency η of the laser defined as the ratio of the laser emission power to the total expended electric power can be represented as

$$\eta = \eta_{\text{KB}} \eta_{\text{K}} \eta_{\text{OHT}} \eta_{\text{P}} \eta_{\text{CO}}, \quad (1)$$

where η_{K} is the vibrational efficiency of the pumping method, i. e. the fraction of power released in the positive discharge column that is expended on excitation of vibrational levels $00^0 1$ of CO_2 and $v=1$ of nitrogen; η_{OHT} is the optical efficiency equal to the fraction of vibrational excitation coupled out of the resonator cavity to molecules that make a transition to the ground state as a result of stimulated emission processes; η_{P} is the efficiency of the discharge circuit, which is equal to the ratio of electric power released in the positive column to the power of discharge supply sources; η_{CO} is the efficiency of the cooling system with consideration of the efficiency of supply sources, as well as power expenditures on producing gas flow and maintaining working pressure. Most publications on gas-discharge lasers represent experimental laboratory research and do not contain information on the optimum values of η_{CO} . Therefore the efficiency of laser systems is frequently characterized by the so-called electro-optical efficiency:

$$\eta_{\text{EO}} = \eta_{\text{KB}} \eta_{\text{K}} \eta_{\text{OHT}}, \quad (2)$$

defined as the ratio of laser emission power to the electric power released in the positive discharge column.

1.1. CO_2 lasers with diffusion cooling of working mixture

Shown in Fig. 2 is a typical diagram of a CO_2 laser with diffusional cooling of the working mixture (diffusion laser) that is the simplest among other laser systems. Usually the diffusion laser consists of a water-cooled discharge tube 1 within which a self-maintained discharge is kept alive by electrode system 2.

18
FOR OFFICIAL USE ONLY

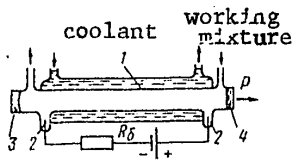


Fig. 2. Construction of laser with diffusional cooling of working mixture

The mirrors of the optical cavity are placed at the ends of the discharge tube: opaque mirror 3, and semi-transparent (or beam-hole) mirror 4. Stability of the laser output characteristics over a prolonged time is maintained by weak circulation of the laser mixture, or by placing a regenerating element inside the sealed-off laser [Ref. 23]. As a rule, diffusion lasers use mixtures of $CO_2:N_2:He = 1:1:3$ or $1:1:6$ (or close to them) at overall pressure $p \approx 10-20$ mm Hg.

Limiting discharge characteristics of the diffusion laser are due to the efficiency of cooling the working mixture ($T_{opt} \sim 250^\circ$), and also the discharge stability. Maximum values of the volumetric energy input due to rate of cooling of the mixture $\langle jE \rangle_{охл}$ can be evaluated from the stationary equation of heat balance in the discharge

$$\langle jE \rangle_{охл} \lesssim \kappa (T_{opt} - T_{ст}) / \Lambda^2, \quad (3)$$

where j and E are the current density and electric field strength in the discharge, $\kappa = cv\rho D$ is the heat conduction of the gas mixture (cv , ρ and D are the specific heat, density and coefficient of diffusion), $T_{ст}$ is the temperature of the cooled wall, $\Lambda = R/2.4$ is the characteristic dimension that determines heat transfer in a cylindrical tube of radius R .

As a rule, pinching of the discharge in the tube is ionization-thermal in nature [Ref. 17, 27]. The increment of development of this instability can be represented as

$$\gamma \approx A \langle jE \rangle / p, \quad (4)$$

where A is a coefficient (~ 10) that is determined mainly by the slope of the curve for the ionization rate constant as a function of parameter E/N (N is the concentration of neutral atoms), p is gas pressure.

The limiting values of $\langle jE \rangle_{уст}$ determined by discharge stability are estimated by setting the increment equal to the characteristic frequency of the process that stabilizes development of this instability. In the diffusion laser such a process is the ambipolar diffusion of charged particles to the walls of the tube. Therefore

$$\langle jE \rangle_{уст} \lesssim p D_a / A \Lambda^2 = D_{a0} p_0 / A \Lambda^2, \quad (5)$$

where D_a is the coefficient of ambipolar diffusion, and D_{a0} is its value at normal pressure p_0 .

Equations (3) and (5) imply that

$$\frac{\langle jE \rangle_{охл}}{\langle jE \rangle_{уст}} \sim \frac{D_a T_r (T_{opt} - T_{ст})}{D_{i0} T_e T_{opt}} A,$$

where T_e is electron temperature, and D_{i0} is the coefficient of ion diffusion at $p = p_0$. Setting $T_e \sim 2$ eV, $T_r \sim T_{opt}$ and $(T_{opt} - T_{ст}) \approx 250$ K, we can readily see

FOR OFFICIAL USE ONLY

that $\langle jE \rangle_{\text{охл}} / \langle jE \rangle_{\text{уст}} \sim 10^{-1}$, and therefore the main process that limits energy input in diffusion lasers is cooling of the mixture.

The limiting power of the diffusion laser can be estimated by the formula

$$P \approx \langle jE \rangle_{\text{охл}} V \eta_{30} \approx \kappa [(T_{\text{opt}} - T_{\text{ст}}) / \Lambda^2] \pi R^2 \eta_{30} L, \quad (6)$$

where V is the volume of the laser tube, L is its length. As can be seen from (6), the quantity P/L for diffusion lasers does not depend on radius of the discharge tube. Substituting the values of heat conduction for He in (6) along with values of $\eta_{30} \sim 0.1-0.2$ that are usual for diffusion lasers, we can estimate the maximum value of power taken from a unit of length of the discharge tube:

$$(P/L)_{\text{дл}} \leq 50-100 \text{ W/m.}$$

The limiting length of the diffusion laser (unless we are considering the waveguide mode) is determined by the diffraction values, and must satisfy the condition

$$L_{\text{дл}} \leq R / 2 \gamma_{\text{диф}} \approx R^2 / 2\lambda, \quad (7)$$

where $\gamma_{\text{диф}} \sim 1.2\lambda/R$ is the diffraction divergence of the laser with wavelength λ . Setting $R \sim 1-3$ cm, we get $L_{\text{дл}} \sim 5-50$ m. Thus the limiting power of the diffusion laser at $R/L \sim 50$ W/m is $P \leq 0.3-3$ kW.

Practically attainable values of $P/L \sim 1-2$ kW have already been achieved in industrial models of diffusion lasers. For example the most powerful Soviet diffusion laser models "Katun'" and "Kardamon" [Ref. 10] consisting of gas-discharge tubes each with $R = 3$ cm and length of 6 m connected in series by a unified optical system provide stable steady-state lasing on the level of $\sim 0.8-1$ kW with specific output of ~ 40 W/m. The laser made by Photon Sources, inc. reaches a power of 1 kW with overall length of six discharge tubes of ~ 13 m; thus $P/L \approx 70$ W/m [Ref. 29].

Let us estimate the limiting values of power density S that can be attained when the radiation of such lasers is focused ($L \sim 1$ kW):

$$S \leq \frac{P}{\pi (\lambda F_m / 2R)^2} \approx \frac{P}{\lambda^2 B} \sim 10 \text{ MW/cm}^2, \quad (8)$$

where $F_m \sim BR$ is the minimum focal length of the lens that permits focusing radiation without spherical aberrations; the coefficient $B \sim 10$. Thus by using the given diffusion lasers we can realistically get output power of ~ 1 kW and power density in the focusing spot of ~ 10 MW/cm²; this limit has already been reached.

A further increase in power of diffusion lasers and reduction of their overall dimensions are possible by using multichannel laser systems proposed in 1970

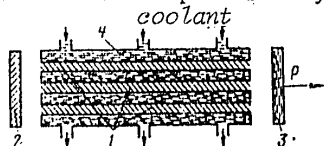


Fig. 3. Diagram of multichannel diffusion laser

[Ref. 30] (Fig. 3). The power increase in such systems is attained by using a large number (N_{Tp}) of parallel discharge tubes or slot discharge gaps 1 joined by two common flat mirrors 2 and 3, one of which (2) is opaque, while the other (3) is semi-transparent. The set of gas-discharge tubes is cooled by circulating coolant 4, and poisoning of the laser mixture is prevented by slow circulation.

Attainment of simultaneous lasing in a large number of parallel laser tubes placed between two flat mirrors that are common to these tubes is much facilitated by the waveguide mode of laser operation, i. e. with satisfaction of the condition

$$R^2/(\lambda L) < 1. \quad (9)$$

Thanks to the parallel placement of the gas-discharge tubes, the multichannel laser system power can be increased to values determined by the possible dimensions of the mirrors and by heat removal from the inside tubes of the laser assembly.

The limiting power of such a laser consisting of a set of cylindrical tubes of length L with inside diameter d and wall thickness δ located a distance Δ apart can be evaluated from the formula

$$P \approx (P/L)_{\text{ДЛ}} L D_0^2 / (d + 2\delta + \Delta)^2, \quad (10)$$

where D_0 is the outside diameter of the laser tube bundle. We can easily see that for realistic overall dimensions of such a device (e. g. $L = 1$ m, $D_0 = 10$ cm, $d = 0.5$ cm and $\delta = \Delta = 0.1$ cm), its power under optimum conditions may reach 5-10 kW, which opens up prospects for creation of high-power miniature laser devices.

The nature of dependence of integrated power of the multichannel laser system on tube diameter at fixed dimensions of the bundle D_0 and L, assuming $\delta = \Delta$, is shown in Fig. 4. The same figure shows experimental values of gain K_0 of the active medium measured at different discharge tube diameters [Ref. 31]. The observed reduction of K_0 at small d may occur if the characteristic time of diffusion and loss of vibrationally excited particles on the walls becomes comparable with the time of their collisional relaxation.

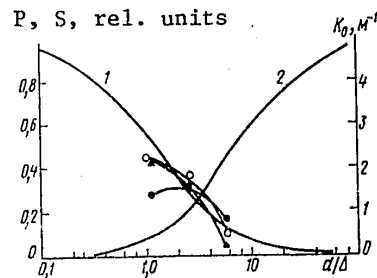


Fig. 4. Dependence of radiation power P (1), power density S in the focal spot (2) and weak signal gain K_0 of active medium of multichannel laser system on discharge tube diameter: $\langle j \rangle = 100$ mA/cm²; mixture CO₂:N₂:He = 1:1:6; p = 20 (●), 30 (○) and 40 (▲) mm Hg

This process may lead to some reduction in P at small d/Δ . The values of optimum d depend on the composition of the mixture and its pressure, and at $p \sim 50$ mm Hg are $\sim 0.2-0.5$ cm [Ref. 31].

If no special steps are taken, each laser tube in the multichannel laser system lases independently of the others. In this case, the divergence of emission of the entire laser system cannot be better than that of one laser tube, and the power density of radiation in the focal spot of the multichannel laser system is

$$S \lesssim \frac{(P/L)_{\text{ДЛ}} L}{\lambda^2 B^2} \frac{d^2}{(d + 2\delta + \Delta)^2} \quad (11)$$

which at $L \sim 1$ m and $(P/L)_{\text{ДЛ}} \sim 10^2$ W/m corresponds to $S \lesssim 1$ MW/cm². The nature of dependence of S on d is shown in Fig. 4 (curve 2). The power density of radiation of the multichannel laser system does not depend on size of the bundle: $P \sim D_0^2$, but the area of the spot in the focal plane of the lens is $\sim D_0^2$ as well (because of the fact that $F_m \sim D_0$) and therefore P cannot be greater than the power density

FOR OFFICIAL USE ONLY

attainable when a diffusion laser of the same length is used, although the integrated power of the multichannel laser system will increase in proportion to D_0^2 .

Radiation density in the focal spot of the multichannel laser system can be increased if all tubes in the bundle can be made to lase coherently. In this case, at least part of the radiation will have divergence corresponding to the diameter of the entire bundle $D_0 \geq d$ rather than to the diameter d of a laser tube.

The possibility of making a multichannel laser system was first demonstrated in 1978 [Ref. 32] as exemplified by an arrangement of 39 parallel laser tubes 1 cm in diameter and about 4 m long placed between flat mirrors: copper (opaque) and KCl single crystal (semitransparent). A special electrode system was used to produce a dc discharge in each of the tubes with specific volumetric energy input of $\sim 2 \text{ W/cm}^2$. The output power of the laser was 3 kW with specific value of $\sim 20 \text{ W}$ from 1 m of each tube.

One of the serious technical problems of making a multichannel laser system with pumping by dc discharge as commonly accepted for diffusion lasers is the introduction of a large number of electrode elements in tubes of small diameter, and ensuring high dielectric strength between a large number of current leads under conditions of tight packing of all tubes. This problem is almost completely eliminated by using electrodeless laser tubes in the multichannel laser system with pumping of the active medium by capacitive ac discharge [Ref. 31]. Studies of the active properties of a medium stimulated by ac discharge with frequency of $f \sim 10\text{--}70 \text{ kHz}$ in tubes were done in Ref. 31. In this paper, besides the dependences of K_0 on p , d , mixture composition and discharge current I , which showed practically no difference from analogous dependences with dc pumping, the authors studied such peculiarities associated with the pumping method as the relation between percentage modulation of output emission $\delta P/P$ and laser working mode, and gave qualitative interpretations of typical curves $\delta P/P \approx f(I, p, f)$ shown in Fig. 5. These characteristics show that the percentage modulation of output emission under optimum working conditions is no more than 5%. Such a value of $\delta P/P$ is not dangerous for most technological applications of the laser.

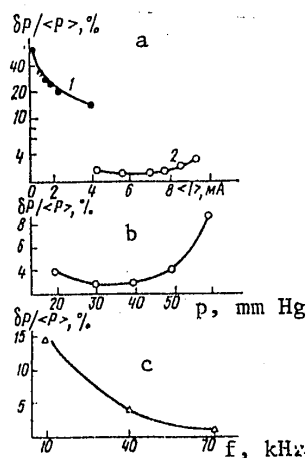


Fig. 5. Dependence of percentage modulation of radiation from the multichannel laser system with ac discharge pumping as a function of discharge current (a), pressure (b) and pumping current frequency (c)

FOR OFFICIAL USE ONLY

The very first experiments demonstrated the feasibility of using ac discharge in multichannel lasers. For example in the MKTL-1 laser [Ref. 84] pumped by ac discharge with frequency of 10 kHz an output power of 1 kW was obtained from a bundle of 61 glass tubes with diameter of 5 mm and length of 1 m, using a germanium output window. The outside diameter of the bundle itself was about 75 mm. The emission divergence of such a laser assembly did not exceed the diffraction divergence of radiation of one laser tube.

The limiting characteristics and structural parameters of the most interesting laser systems with diffusional cooling of the working mixture are summarized in Table 1. As we can see from this table, even at a very low specific power output $P/(N_{TP}l_{TP})$, multichannel lasers enable an appreciable increase in the power taken from a unit of structural length of the laser ($\sim l_{TP}$). There is a concomitant sharp reduction in the number of mirrors used and in the transverse dimensions of the structure.

TABLE 1
Characteristics of process lasers with diffusion cooling of mixture

Name (company)	Pumping method	P, kW	l_{TP}/N_{TP} , m/tube	N_m	$P/(N_{TP}l_{TP})$, W/m	P/l_{TP} , W/m	Ref.
M-400 (Ferranti)	SMDCD	0,4	1,5/12	13	22	266	[8]
Kardamon	SMDCD	0,9	6/4	8	38	150	[10]
Photon sources inc.	SMDCD	1,0	2,2/6	7	75	450	[29]
Iglan	SMDCD	3,0	4/39	2	19	750	[32]
MKTL-1	ACD	1,0	1/60	2	15	1000	[84]

Notes: P--laser power; l_{TP} --length of discharge tube; N_{TP} --number of discharge tubes; N_m --number of mirrors in optical cavity; SMDCD--self-maintained dc discharge; ACD--ac discharge.

1.2. Fast-flow CO₂ gas-discharge lasers

Significant progress in increasing the power of electric-discharge lasers became possible as a result of utilizing convective cooling, i. e. rapid circulation of the working mixture through the discharge zone [Ref. 43]. Such lasers are called fast-flow electric-discharge lasers or lasers with convective cooling. The ratio of the rate of convective heat transfer to the rate of diffusional cooling is equal to the ratio of the diffusion time τ_D to the time of gas travel through the discharge zone τ_c :

$$\tau_D/\tau_c \approx \Lambda^2 M / l \lambda_T, \quad (12)$$

where λ_T is the mean free path of molecules; Λ is a characteristic dimension that determines the rate of heat diffusion (in a diffusion laser $\Lambda \sim R/2.4$); l is the length of the discharge zone along the flow; M is the Mach number for the gas flow.

Rapid gas flow along the optical axis of the laser (see Fig. 1) gives appreciable advantages over the diffusion laser. However, the considerable length l of the

FOR OFFICIAL USE ONLY

active zone that is necessary for efficient operation of the cavity precludes making the quantity τ_c sufficiently small, and makes it difficult to produce a high gas flowrate. Therefore, even though the specific power output of such systems has been increased from 50-100 to 500-1500 W/m, the limiting power of the laser has been raised only to 2-6 kW [Ref. 8, 29].

Much more promising is circulation of the gas in the direction perpendicular to the optical axis of the laser (diagram III of Fig. 1). In this case the length of the optical axis is not associated with the length of the pumping zone in the direction of the flow, and therefore, substituting values of $M \sim 0.1-1$, $\Lambda \sim 7-10$ cm, $\lambda_T \sim 10^{-4}$ cm that are typical of convective lasers in (12) (at $p \sim 0.1$ atm), we readily see that the rate of heat transfer in convective lasers may be 4-5 orders of magnitude greater than those in diffusion lasers. For this reason, the main factor that influences the limitation on specific power $\langle jE \rangle$ invested in the discharge of the convective laser becomes discharge stability.

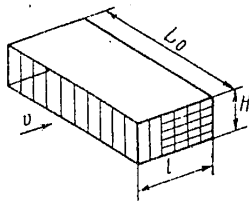


Fig. 6. Diagram of CO₂ fast-flow gas-discharge laser; vertical shading denotes the pumping zone, horizontal shading shows the cavity

The power of convective lasers with transverse circulation, illustrated by the general diagram of Fig. 6, is determined by the total flowrate of gas mixture through the laser, the admissible heating temperature of the mixture $T_T \sim T_{O, \pm} \sim 150^\circ\text{C}$, and by the electro-optical efficiency η_{EO} of the pumping method:

$$P_{\text{KП}} \approx w_g \rho H L_0 v \eta_{\text{EO}}, \quad (13)$$

where $w_g = (T_{\text{opt}} - T_0)C$ is limiting mass energy input; T_0 is the gas temperature at the input to the pumping zone; C and ρ are the specific heat and specific density of the mixture; v is the rate of circulation; H and L_0 are the altitude of the pumping zone and its length along the optical axis. Substituting values of parameters that are typical of convective lasers with different pumping methods: $w_g \approx 200-300$ J/g (depending on the composition of the mixture), $\rho \sim (1-10) \cdot 10^{-5}$ g/cm³, $H \sim 10$ cm, $v \sim 10^2$ m/s and $\eta_{\text{EO}} \sim 0.1-0.2$, we readily see that values of $(P/L_0)_{\text{KП}} \sim 1-100$ kW/m are possible under conditions of convective lasers. In the case of diffusion lasers, the limiting values of $(P/L_0)_{\text{ДЛ}}$ were determined only by the admissible heating of the working mixture. For convective lasers, the quantity P/L_0 depends on structural and operational parameters and to a great extent is determined by the type of gas discharge used for stimulating the medium. The limiting values of power density in the focal spot of the convective laser in this case are

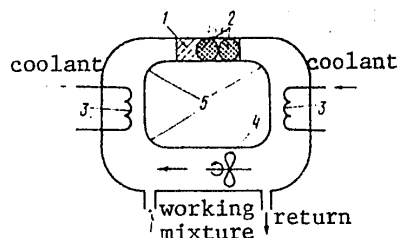
$$S = \frac{(P/L_0)_{\text{KП}} L_0 \beta^2}{\lambda^2 \beta^2} \leq (10-1000) \dot{L}_0 \text{ [m], MW/cm}^2, \quad (14)$$

where $\beta < 1$ is a geometric coefficient that depends on the type and transparency of the optical cavity used (usually $0.1 \leq \beta < 1$).

A considerable disadvantage of the convective laser is the necessity for circulating a large quantity of working mixture. In the diffusion laser, the rate of circulation was determined by the rate of chemical poisoning of the mixture,

and could even be zero with regenerators present. On the other hand, in the convective laser it is necessary to circulate 20-50 g/s of mixture through the cavity for every kilowatt of laser power.

Development of stationary high-power convective process lasers with dumping of depleted mixture (open-cycle convection lasers) is inadvisable from the economic standpoint, and difficult to realize at high power levels from the technical standpoint. Therefore as a rule circulation of the working mixture in high-power convective lasers is usually through a closed gasdynamic channel (closed-cycle convection laser). A typical diagram of such a laser is shown in Fig. 7. It consists of a gas-discharge chamber 1, optical cavity 2, heat exchangers 3, mixture circulation unit 4 and gas lines 5 that connect them. Stability of properties



of the active medium under conditions of the closed-cycle convection laser is maintained by continuous renewal of a small portion of the mixture (0.1-1% of the flowrate in the loop) or by regenerators located in the loop [Ref. 13].

The dimensions of the discharge zone l in the direction of gas flow depend on the gasdynamic parameters of the working medium and the limiting volumetric energy inputs $\langle jE \rangle$ of the pumping method:

$$l \approx w_g \rho v / \langle jE \rangle. \quad (15)$$

Fig. 7. Typical diagram of a closed-cycle convection laser

If the vibrational energy stored on levels $(00^0 1)$ of CO_2 and N_2 has time to relax in collisions during the time of gas transit through the discharge ($l \gtrsim v/v_r$, where v_r is the relaxation frequency), the cavity zone must be partly or almost completely coincident with the pumping zone. Such electro-optical schemes, so-called combined-cavity schemes, are the most widely used in closed-cycle convection lasers. If $l \lesssim v/v_r$, the cavity can be placed directly after the gas-discharge chamber (separated-cavity scheme). Such arrangements may be advisable if resonator combination is impossible because of the structural peculiarities of the gas-discharge chamber [Ref. 34]; however, they are rarely used in closed-cycle convection lasers. Their use is frequently justified under conditions of open-cycle convection lasers, particularly in electric-discharge arrangements with admixing of the CO_2 before the optical cavity. A diagram of such a laser is shown in Fig. 8. Absence of CO_2 in the discharge zone sharply reduces v_r and enables operation at elevated pressures (up to ~ 100 mm Hg) under conditions of long discharge chambers. Because of this, CO_2 discharge lasers of high power can be made. However, as a rule because of the limited reserve of working mixture and difficulties with organizing circulation, such systems operate under quasi-steady state conditions.

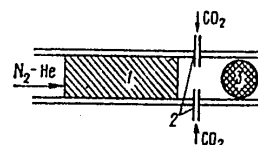


Fig. 8. Diagram of open-cycle electric discharge laser with admixing of CO_2 preceding the cavity: 1--pumping zone (gas-discharge chamber); 2-- CO_2 delivery system); 3--optical cavity zone

2. Methods of pumping gas-discharge lasers

Extensive use of self-maintained and semi-self-maintained discharges in cool gas for pumping powerful CO_2 lasers is due to high efficiency of stimulating

FOR OFFICIAL USE ONLY

molecular vibrations in collisions of molecules of working mixture with plasma electrons. Maximum vibrational efficiency $\eta_K \approx 0.9$ is reached at values of the average energy of electrons corresponding to values of the "normalized" electric field $E/N \approx (1.5-2) \cdot 10^{-16} \text{ V} \cdot \text{cm}^2$ [Ref. 35, 36] (N is gas molecule concentration) and not supporting self-maintained ionization of the gas, i. e. under semi-self-maintained discharge conditions. Under self-maintained discharge conditions (at $E/N \approx (3-5) \cdot 10^{-16} \text{ V} \cdot \text{cm}^2$), the value of η_K is somewhat reduced, but still remains fairly high ($\eta_K \approx 0.75-0.85$) [Ref. 35, 36], which makes the self-maintained discharge an attractive pumping method as well.

Studies of the physical and technical aspects of different discharge types to find the simplest and most efficient methods of pumping have been intensively done for the last decade. Let us consider the most well developed and efficient methods.

2.1. Self-maintained dc discharge

Currently, the most extensively used method of pumping convective lasers and the simplest from the standpoint of technical realization is the self-maintained dc discharge. Depending on the direction of the electric field vector with respect to gas flow, lasers with longitudinal and transverse discharges are distinguished. Typical diagrams of gas-discharge chambers with self-maintained dc discharge are shown in Fig. 9.

The mechanism of closure of direct current flowing in the gas stream is satisfactorily described by the classical theory of a glow discharge with cold cathode [Ref. 37]. Under ordinary conditions of CO₂ laser operation the current density in the glow-discharge volume is 1-2 orders of magnitude lower (depending on the pressure and composition of the mixture) than the normal current density on the cathode. Therefore cathodes 3 of the gas-discharge chamber are made in the form of small emitting sections of elongated or circular shape uniformly distributed over dielectric cathode plate 2. The overall area of these sections is less than the area of the discharge dimension transverse to the current. In the case of a transverse discharge, the cathodes may protrude into the gas flow in the form of pins [Ref. 38], or may be on one level with the cathode plate [Ref. 39]. In the case of a longitudinal discharge, the cathodes are made in the form of pins or needles uniformly located in the cross section of the gas flow [Ref. 40].

To facilitate discharge ignition and keep it stable and homogeneous in the volume of the gas-discharge chamber with electric supply from one source, there is a ballast resistor R_b in the circuit of each cathode element across which from 20 to 50% of the voltage of the supply source is lost in the case of a transverse discharge [Ref. 12, 34], and ~10% with longitudinal current flow [Ref. 40].

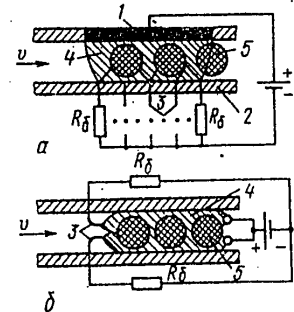


Fig. 9. Diagrams of laser gas-discharge chambers with longitudinal (a) and transverse (b) self-maintained dc discharge: 1--anode; 2--cathode plate; 3--cathode; 4--pumping zone; 5--cavity zone

In most research, anode 1 is continuous and equipotential [Ref. 11, 12, 40]. In some gas-discharge chamber designs, transverse self-maintained dc discharge is made homogeneous by sectionalizing the anode with an equipotential cathode [Ref. 5] or by sectionalizing both electrodes [Ref. 42].

Let us take up the principal characteristics that determine the outlook for using this type of discharge for pumping convective lasers. Usually self-maintained dc discharges with transverse or longitudinal flow of discharge current have weakly rising or nearly horizontal current-voltage curves. The quantity E/N is $(4-6) \times 10^{-16} \text{ V}\cdot\text{cm}^2$. With transverse current flow, the electric field strength decreases along the gas stream, and may change by a factor of 1.5-2 within the gas-discharge chamber [Ref. 34, 43, 44]. This situation is also one of the reasons for sectionalizing the cathodes and providing them with individual ballast resistors.

Experimental research on energy balance in the positive column of a self-maintained dc discharge has been done only for nitrogen and air [Ref. 44-46]. According to this research, the value of η_K in a mixture of air with CO_2 falls from 0.85 to 0.6 as the gas pressure increases from 40 to 80 mm Hg [Ref. 46]. At $p = 40-60$ mm Hg, 5-10% of the energy released in the positive column is expended on excitation of rotational levels of N_2 and O_2 , and at $p = 70-100$ mm Hg--10-25% [Ref. 44, 45]. The remaining energy is apparently expended on excitation of electronic metastable states and plasma-chemical reactions, the relative contribution of these as yet little investigated loss channels increasing with an increase in the pressure of the mixture. Theoretical calculations of the energy balance in a self-maintained dc discharge for a laser mixture at $E/N \approx (4-5) \cdot 10^{-16} \text{ V}\cdot\text{cm}^2$ give $\eta_K = 0.9$ and $\eta_T = 0.1$ [Ref. 36].

Let us compare the values of pumping efficiency for longitudinal and transverse discharges from the electrical engineering standpoint, taking values of $E/N \sim 4 \cdot 10^{-16} \text{ V}\cdot\text{cm}^2$, $p \sim 30$ mm Hg, $H \sim 5$ cm and $L \sim 50$ cm that are typical of gas-discharge chambers with self-maintained dc discharge. Assuming overall losses in the electrode region of 400 V and percentage of source voltage lost on the ballast resistors of ~30-50% for transverse discharges, and ~10% for longitudinal discharges, we readily get the efficiencies of the discharge circuit: $\eta_{p\parallel} \sim 0.9$ [Ref. 40, 41] for longitudinal current flow, and $\eta_{p\perp} \sim 0.4-0.6$ [Ref. 5, 11, 12] for transverse. It is the low values of η_p that explains the considerable difference between η_{30} and η observed in Ref. 12, 34 for convective lasers with pumping by transverse self-maintained dc discharge. Despite high values of $\eta_{30} \sim 0.15$ [Ref. 11, 12], the overall efficiency of such devices usually does not exceed $\eta \sim 0.05-0.07$ [Ref. 5, 12].

As has been demonstrated above, the overall dimensions of the gas-discharge chamber depend on the limiting values of volumetric specific energy inputs $\langle jE \rangle$ that are restricted in the case of convective lasers by formation of pinches [Ref. 17, 18, 47, 48]. The reason for plasma pinching can be found in various instabilities of overheating nature [Ref. 16-18] that are intensified in self-maintained discharges due to positive feedback between energy release in the gas and ionization processes.

The limiting values of $\langle jE \rangle$ at low pressures can be estimated by setting the time of development of the overheating instabilities of the self-maintained discharge

FOR OFFICIAL USE ONLY

TABLE 2
 Characteristics of gas-discharge chambers [GDC]
 with transverse circulation

Pumping method	GDC dimensions, cm			p, m/s	p, mm Hg	Mixture CO ₂ :He:N ₂	$\langle jE \rangle$, 3		p _p	Used in	Ref.
	H	L ₀	l				W/cm ²	w _g , J/s			
Transv. SMDCD	4	100	15	50	18	2:11:5	1,4	140	0,5	CCCL	[5]
Ditto	4	90	20	80	50	1:20:20	5,5	320	0,5	Ditto	[11]
•	6	130	35	90	25	1:17:0+2 parts air	2,5	240		•	[12]
Longit. SMDCD	5,6	76	100	240	37	2:5:30	1,9	360	0,9	•	[52]
Longit. SMDCD and transv. ACD	6,3	240	53	130	30	1:6:12	2,0	400	0,9	•	[24]
Transv. NDEB	10	100	20	90	50	1:28:16+0,6 Xe	4,5	170	0,85	•	[13]
Transv. NDEB	3,3	15	3	150	150	1:30:15	160	200		Pilot OCCL	[65]
Longit. NDIP	5,5	76	67	220	30	1:7:12	2,2	280	0,85	CCCL	[60,72]
Trans. NDIP	10	15	23	60	45	1:30:30	5	450	0,83	Pilot OCCL	[67,71]
Transv. ACD	10	15	20	100	50	1:10:9	7	300	0,9	Pilot OCCL	[85,86]

Note: H, L₀ and l are the height, width and length of the discharge gap; $\langle jE \rangle$ and w_g--averaged specific volumetric and mass energy inputs; SMDCD--self-maintained dc discharge; ACD--ac discharge; NDEB--non-self-maintained discharge kept alive by electron beam; NDIP--non-self-maintained discharge kept alive by periodic ionization pulses; CCCL--closed-cycle convective laser; OCCL--open-cycle convective laser

(ionizational-superheating, ionizational-excitation, see (4)) equal to the time of transit of the mixture through the discharge zone:

$$\langle jE \rangle_{np} \approx Pv/AI. \tag{16}$$

Estimates made by using relation (16) differ sharply from experimental data at p ≥ 30 mm Hg. Special studies [Ref. 49, 50] have shown that under these conditions the pinch may develop in the anode region rather than in the body of the plasma, and then propagate toward the cathode like a streamer at a velocity of ~10⁴-10⁵ cm/s. In this case $\langle jE \rangle$ does not increase linearly with P, but remains constant or falls [Ref. 43].

Currently there is no theory that gives one-to-one relationships between $\langle jE \rangle_{np}$ and gasdynamic parameters of the flow or geometric characteristics of the gas-discharge chamber. Therefore the $\langle jE \rangle_{np}$ necessary for calculating convective lasers must be taken from experiment.

In the case of a transverse discharge, it has been shown by experiments [Ref. 5, 11, 12, 34, 43] that $\langle jE \rangle_{np}$ changes in the following way: 1) increases with pressure up to $p \sim 20-40$ mm Hg, and then saturates or begins to decrease; 2) increases with gas velocity up to $v \sim 50-100$ m/s, and then saturates or begins to fall; 3) decreases with increasing height H of the discharge gap; 4) beginning at a certain length, decreases with increasing l (there is no additivity of the contribution in the direction of flow); 5) increases with addition of He to the mixture; 6) decreases with increasing CO_2 content and H_2O in the working mixture. Specific mass energy inputs w_g in a gas-discharge chamber with self-maintained dc discharge decrease with increasing pressure, and increase with increasing l [Ref. 12, 34, 43].

Typical characteristics of gas-discharge chambers with self-maintained dc discharge are summarized in Table 2.

Most gas-discharge chambers with transverse discharge use mixtures that contain helium; at partial pressure of nitrogen not exceeding 30 mm Hg, and total pressure p of the mixture of the order of 50 mm Hg or less, flowrate of 30-100 m/s, $H = 3-6$ cm and $l \sim 20-40$ cm, we can get $\langle jE \rangle_{np} \sim 2-5$ W/cm³ at $w_g \sim 250-300$ J/g in helium mixtures, and 150-250 J/g in helium-free mixtures. Because of the high cost of helium, the use of helium-free mixtures is of particular interest for lasers with partial renewal of the working mixture.

Substituting typical values of $\langle jE \rangle_{np}$ in (15), we get $l > v/v_r$ for a gas-discharge chamber with self-maintained dc discharge, and therefore high η_{30} can be achieved only by using a combined cavity scheme. Since the diameter of mirrors used in the laser $D \sim H < l$, resonators of convective lasers with pumping by self-maintained dc discharge are nearly always multipass [Ref. 5, 11, 12].

At the present time the characteristics of longitudinal self-maintained dc discharges have not been adequately studied. For laser mixtures we have only isolated values of $\langle jE \rangle_{np}$ obtained for fixed conditions [Ref. 24, 40, 51]. As a rule, these experiments were done at high flowrates (of the order of 100 m/s or more), $l \sim 40-50$ cm, and in the absence of special steps to achieve stabilization were distinguished by comparatively low values of $\langle jE \rangle \lesssim 1$ W/cm³. Higher values (5 W/cm³) were attained in studying self-maintained dc discharge in an air flow at pressure of 40-60 mm Hg [Ref. 26]. Just as in the case of transverse self-maintained dc discharge, $\langle jE \rangle$ and w_g in the longitudinal self-maintained dc discharge decrease with increasing l [Ref. 26, 51] and pressure of the working mixture [Ref. 51]. Nonmonotonic dependence of $\langle jE \rangle$ on air flowrate in such a discharge is noted in Ref. 51.

In laser devices that use longitudinal self-maintained dc discharge for pumping, the quantity $\langle jE \rangle$ can be increased by additional gasdynamic or electrical action on the discharge.

Stabilizing the discharge by gas flow involves more than mere limitation of the time that the gas stays in the discharge zone. Since the plasma electrons are bound by electrostatic forces to ions, and the latter--due to collisions--are bound to neutral gas molecules, discharge stability may be influenced by controllable changes in the gasdynamic flow parameters (in particular by turbulence intensity). The gasdynamic action of gas flow on a discharge was studied in Ref. 26,

29
FOR OFFICIAL USE ONLY

FOR OFFICIAL USE ONLY

52-60. The authors of Ref. 53-56 made an attempt to find a relation between observed electric characteristics of the discharge and the Reynolds number of the flow. In Ref. 53, an abrupt change in the discharge burning conditions was observed at $Re \geq Re_{cr}$. In Ref. 56 an effect of discharge decontraction was observed upon transition to turbulent conditions. The independent change in degree of flow turbulence by turbulizing grids [Ref. 57, 58] enabled separation of effects of stabilization by convection and turbulence. In Ref. 26, 57, the significance of homogeneity of the flow velocity profile was noted in addition. A qualitative effect of the influence of turbulence scale on discharge stability was observed in Ref. 59. A quantitative investigation of the influence of controllable degree of flow turbulence at limiting values of $\langle jE \rangle$ in a longitudinal self-maintained dc discharge has been carried out in air at $p = 40-60$ mm Hg [Ref. 26]. It was shown (Fig. 10) that controllable flow turbulence set up by a special grid with coef-

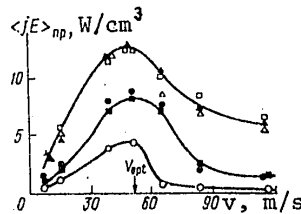


Fig. 10. Limiting power invested in longitudinal self-maintained dc discharge as a function of flow velocity and degree of turbulence of the medium: $p = 50$ mm Hg; $l = 10$ cm; $H = 6$ cm; $D_T/v = 0.25 \cdot 10^{-2}$; $\epsilon = 0.05$ (■), $0.05 \cdot 10^{-2} - 0.12$ (●), $2 \cdot 10^{-2} - 0.18$ (○), $3 \cdot 10^{-2} - 0.22$ (▲), $4.5 \cdot 10^{-2} - 0.26$ (△), $7 \cdot 10^{-2} - 0.3$ (□) [Ref. 26]

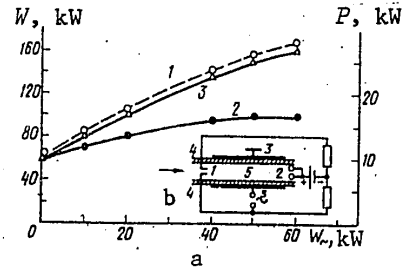


Fig. 11. Emission power (1), power invested in the dc discharge (2) and total discharge power (3) as functions of the auxiliary rf discharge power (a) for $CO_2:N_2:He = 1:6:12$, $p = 30$ mm Hg, $v = 130$ m/s, and diagram of the experiment (b): 1--cathode; 2--anode; 3--ac voltage supply; 4--dielectric plate; 5--discharge zone

efficient of turbulent diffusion D_T depending on its scale may either increase or reduce $\langle jE \rangle$; in optimum modes when the effect of turbulent stabilization was comparable with or greater than the effect of stabilization by convective entrainment, the quantity $\langle jE \rangle$ could rise by a factor of 2-4. High efficiency of gasdynamic action of the flow on discharge in a laser mixture was also demonstrated in Ref. 52, 60.

Superposition of an auxiliary rf field on the discharge that is transverse with respect to the main field may also lead to decontraction of the plasma and an increase in $\langle jE \rangle_{np}$ in longitudinal self-maintained dc discharges [Ref. 24, 51, 62]. In laser devices this effect was first demonstrated in the gas-discharge chamber shown in the diagram of Fig. 11 [Ref. 24, 51]. Switching on an alternating field with frequency of 13.5 MHz tripled the power invested in the discharge, and the combined gasdynamic and electrical action on the discharge raised $\langle jE \rangle_{np}$ to about $2 W/cm^3$. According to theoretical studies [Ref. 62, 63] superposition of rf fields on a self-maintained dc discharge can increase $\langle jE \rangle_{np}$ by a factor of 1.1-1.5.

TABLE 3
 Characteristics of closed-cycle convection laser
 with transverse circulation

Name (company)	Pumping method	P, kW	P/L ₀ , kW/m	P/Q _v , J/g	P/G, J/g	$\eta_{30}\eta_p$	Ref.
Experimental Facility	Transv. SMDCD	1	1	0,4	15	0,06	[5]
GTE 973 (Silvania)	»	3	3,3	1,3	60	0,06	[42]
LT-1	»	5	5,5	1,8	35	0,06	[11]
CL-5	»	5	5	—	—	0,07	[8]
TL-10	»	10	7,7	1,4	36	0,08	[12]
Mitsubishi	»	1,5	0,9	1,7	17	—	[9]
Experimental facility (CO ₂ amplifier)	Longit. SMDCD	19	25	2,5	100	0,21	[52]
Ditto	Longit. SMDCD & transv. ACD	27	11,2	1,3	67	0,15	[24]
HPL-10 (Avco-Everett)	Transv. NDEB	15	15	—	—	—	[6]
CO ₂ EI-laser	Transv. NDEB	10	10	1,1	20	0,09	[13]
Tsiklon	Longit. NDIP	6	7,9	0,7	31	0,09	[72]

Note: P--Laser power; L₀--dimension of gas-discharge chamber in direction of optical axis; Q--volumetric flowrate of mixture in loop, m³/s; G--mass flowrate of mixture in loop, g/s

Characteristics of the most interesting laser devices that use transverse and longitudinal self-maintained dc discharges for pumping are summarized in Table 3. Besides output power and the quantity $\eta_{30}\eta_p$ that is close to the total efficiency of the laser (usually $\eta \sim (0.8-0.9)\eta_{30}\eta_p$), this table contains data on a most important dimension L₀ that to a great extent determines the overall dimensions of the entire device; this is the length of the gas-discharge chamber across the flow. The table also summarizes data on the volumetric and mass flowrates of the mixture in a closed loop. The working conditions for gas-discharge chambers used in many devices are given in Table 2. It should be noted that practically all modern laser facilities operate on working mixtures with a high helium content. An exception is the TL-10 [Ref. 12] that uses a mixture of CO₂ with nitrogen and air. All lasers with self-maintained dc discharge operate at comparatively low pressures (the partial pressure of nitrogen does not exceed 20-25 mm Hg) and at volumetric energy inputs of 2-5 W/cm³, and can yield electro-optical efficiency of 15-25%. The overall efficiency of a convective laser with transverse pumping by self-maintained dc discharge is less than ~0.1, which is due to the low value of η_p . In the case of longitudinal discharge, $\eta_p\eta_{30}$ may reach ~0.2. The power taken from a unit of length of the laser along the optical axis is 1-8 kW/m for transverse pumping, and 10-25 kW/m for longitudinal pumping. This considerable difference can be attributed to the high flowrates in longitudinal systems. The values of output power normalized to the volumetric flowrate of the device are 1-2 kW/m³/s in either case. In lasers intended for use in industry where closed loops with a high rate of circulation are inadvisable from the economic standpoint because of rising hydraulic losses [Ref. 13], realistic values of P/L₀ are of the order of 10 kW/m or less.

31
 FOR OFFICIAL USE ONLY

FOR OFFICIAL USE ONLY

In estimating prospects for raising power in laser devices with self-maintained dc discharge, we can expect that for reasonable and realistically attainable values of $L_0 \sim 2$ m and $v \sim 100$ m/s the power of a convective laser in the case of transverse pumping will be limited on a level of 10 kW due to difficulties associated with organizing the discharge at $H \geq 5$ cm. Longitudinal discharge is less sensitive to the quantity H , and therefore it is to be hoped that the output power of the laser will increase in proportion to H . However, in experimental devices with longitudinal self-maintained dc discharge, $H \leq 6$ cm.

2.2. Semi-self-maintained discharge with electron-beam ionization

The semi-self-maintained discharge can optimize the parameter E/N in the gas-discharge chamber of convective lasers for pumping of the working medium, and therefore this discharge has a maximum value of η_K of the order of 0.9 or more [Ref. 35, 36]. Another advantage of the non-self-maintained discharge is higher stability than the self-maintained dc discharge associated with a sharp reduction in the increments of instabilities of the ionization-superheating type at values of E/N 1.5-2 times lower than for self-maintained dc discharges. At the present time the best developed equipment is for the non-self-maintained discharge kept alive by electron beam [NDEB], and the prospects for further increase in power in process lasers are tied up with this type of discharge.

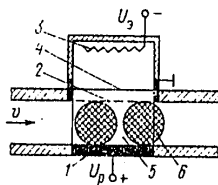


Fig. 12. Diagram of gas-discharge chamber of laser with pumping by NDEB: 1--gas-discharge chamber anode; 2--GDC cathode; 3--electron gun cathode; 4--foil; 5--pumping zone; 6--optical cavity zone

A typical diagram of a gas-discharge chamber for pumping the working medium of a laser with NDEB is shown in Fig. 12. The working medium is ionized by a beam of fast electrons introduced into discharge gap 5 from an electron accelerator through thin metal foil 4. The average energy of the plasma electrons is determined by the magnitude of the constant electric field maintained between grid-cathode 2 and anode 1 of the discharge gap. The homogeneous beam of accelerator electrons with energy of 100-250 keV and current density of the order of $10 \mu\text{A}/\text{cm}^2$ or more provides a homogeneous non-self-maintained discharge, and consequently gives high uniformity of optical properties of the active medium.

The physical processes in the NDEB and its parameters have been quite intensely studied over the last decade [Ref. 13, 19, 64-66]. Therefore we will take up only the major aspects of this research that are of practical interest to laser technology.

Questions of NDEB stability are studied in detail in the survey of Ref. 19. In particular, it is shown in this paper that maximum energy inputs to the NDEB may be limited by development of volumetric superheating instabilities, as well as instabilities due to phenomenon near the electrodes [Ref. 66].

Typical current-voltage curves of the NDEB are rising, and therefore the electrodes and ballast resistors need not be sectionalized to ignite and maintain the discharge. The potential drop near the electrodes in the NDEB is 400-500 V [Ref. 13, 65]. In contrast to the self-maintained dc discharge, the quantity $\langle jE \rangle$ in the

NDEB increases linearly with increasing flowrate [Ref. 13] and mixture pressure [Ref. 13, 65], i. e. the current density j_{np} of transition to arcing is independent of pressure up to ~300 mm Hg [Ref. 19, 65]. The limiting values of $\langle jE \rangle$ in the NDEB in nitrogen at $p = 150$ mm Hg reach ~ 200 W/cm³ at $j \sim 300$ mA/cm² [Ref. 65]. Even in facilities of industrial scale, values of $j \sim 25$ mA/cm² are reached at $\langle jE \rangle \sim 5$ W/cm³ [Ref. 13].

The non-self-maintained discharge also has advantages over the self-maintained dc discharge in the energy balance in the discharge. As indicated above, at optimum E/N, 90-95% of the energy invested in the positive column of the semi-self-maintained discharge is expended on exciting vibrational levels of nitrogen ($\eta_n \sim 0.9-0.95$) [Ref. 36, 45]. Expenditures on direct heating of the mixture at $E/N \approx (1.5-2) \cdot 10^{-16}$ V·cm² in this case do not exceed $\eta_K = 0.05$ [Ref. 45, 67]. Since the energy released in the electrode layers of the NDEB at typical values of $H \sim 10$ cm does not exceed ~10%, while expenditures on creating the electron beam are 5-10% [Ref. 13, 19, 65] of the W_{nc} , the efficiency η_p of the discharge circuit of the NDEB should be 0.8-0.85. The possibility of attaining high values of $\langle jE \rangle$ of the order of 100 W/cm³ or more at elevated pressures ($p \gtrsim 150$ mm Hg) opens up real prospects for reducing the overall dimensions of laser devices, raising their power, and simplifying electro-optical arrangements.

The parameters of gas-discharge chambers and laser devices with NDEB are summarized in tables 2 and 3. Values of $\langle jE \rangle$ and P near the maximum for lasers with self-maintained dc discharge have already been achieved in devices of this type.

In speaking of the operational peculiarities of lasers with NDEB, it must be noted that the presence of a high-voltage (up to 250 kV) and high-current ($10^{-1}-10^{-2}$ A) electron accelerator not only complicates construction and operation of the facility, but requires effective biological shielding for service personnel.

2.3. Semi-self-maintained discharge with ionization by periodic pulses

The above mentioned technical and operational complexities of realizing NDEB can be obviated in great measure by using a non-self-maintained discharge kept alive by periodic ionization pulses [NDIP] for pumping CO₂ lasers. This is often called a combined discharge in the literature. Use of this type of semi-self-maintained discharge for pumping a laser medium was first suggested in 1972 [Ref. 68, 69]. The working principle of such a discharge is illustrated in Fig. 13a. Conductivity of the gas in the NDIP is maintained by ionization that takes place in the volume under the action of high-voltage ($E/N \sim (1-2) \cdot 10^{-15}$ V·cm²) periodic pulses of short duration ($\tau_n \lesssim 0.1$ μ s) at recurrence rate of $f_n \sim 1-100$ kHz. In the period between two successive ionization pulses, a non-self-maintained current flows in the decaying plasma, kept alive by a constant voltage U_p applied across the discharge gap, corresponding to the value of parameter E/N that is optimum for excitation of the active medium. The ionization pulse recurrence rate must exceed the characteristic frequency of plasma decay, i. e. it must satisfy the condition

$$f_n \gg \beta_0 n_0, \quad (17)$$

where β_0 is the effective recombination coefficient at optimum $E/N \sim (2-3) \cdot 10^{-16}$ V·cm², $\beta_0 \sim 10^{-7}$ [Ref. 70]. Therefore condition (17) at $n_e \sim 10^{10}$ cm⁻³ takes the form $f_n \gg 1$ kHz.

FOR OFFICIAL USE ONLY

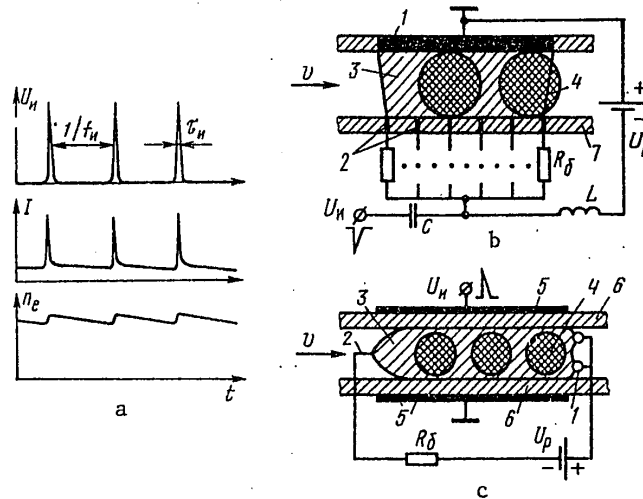


Fig. 13. Time dependences of pulsed power supply voltage U_H , discharge current I , and electron concentration n_e (a), and diagrams of gas-discharge chambers (b, c) with pumping by NDIP: 1--anode; 2--cathode; 3--discharge zone; 4--optical cavity zone; 5--grid; 6--dielectric wall; 7--cathode plate

The outlook for using such a discharge in laser technology has been studied on the two types of gas-discharge chambers shown in Fig. 13b, c. In the first of these, constant and pulsed electric fields are set up by the same electrode system and directed perpendicular to the gas flow and to the direction of the optical axis (transverse version) [Ref. 71]. The electrode system consists of continuous anode 1 and a set of copper pin cathodes 2 set flush with cathode plate 7, each pin being connected to a source of constant voltage through ballast resistor R_δ . The inductance in the dc circuit protects the source of constant voltage from high-voltage ionizing pulses.

In the second type of gas-discharge chamber for NDIP [Ref. 72] the constant electric field is directed contrary to the gas flow, and as in the gas-discharge chamber for longitudinal self-maintained dc discharge [Ref. 40], it is maintained between pin cathodes 2 protruding into the flow and tubular anodes 1 (longitudinal version). The pulsed ionizing discharge is capacitive and is realized through dielectric walls 6 of the gas-discharge chamber by means of metal grids 5 placed on the outside of the walls. The pulsed electric field is directed perpendicular to the gas stream.

The proposed versions of gas-discharge chambers can set up a homogeneous discharge with optimum E/N in large volumes (1-20 liters). Just as in the case of the NDEB, the current-voltage curve of the NDIP is rising [Ref. 60, 72], enabling a reduction in values of ballast resistors as compared with the self-maintained dc discharge. The optimum frequencies of ionizing pulses are different for the two types of gas-discharge chambers, being 2-4 and 70 kHz for the variants of Fig. 13b, c respectively [Ref. 67, 72]. Studies have shown that NDIP is more stable than self-maintained dc discharge, and for laser mixtures gives maximum

34
FOR OFFICIAL USE ONLY

$\langle jE \rangle \approx 5-10 \text{ W/cm}^3$ and $w_g \sim 250-450 \text{ J/g}$ in the transverse version of the gas-discharge chamber [Ref. 67], and also $\langle jE \rangle \approx 1.6 \text{ W/cm}^3$ and $w_g \sim 210 \text{ J/g}$ in the longitudinal version [Ref. 60]. This enables an increase in the interelectrode gap to $H \sim 10 \text{ cm}$ and a reduction in the length of the discharge zone with some increase in pressure of the working mixture [Ref. 67]. Studies of the energy balance in the transverse version of NDIP [Ref. 67] have shown that the values of vibrational efficiency may exceed 0.9 in pure nitrogen, and reach $\eta_K \sim 0.9 \pm 0.05$ at $E/N = 1.25 \cdot 10^{-16} \text{ V}\cdot\text{cm}^2$ and $w_g \sim 250 \text{ J/g}$ in the laser mixture [Ref. 67]. The fraction of energy that goes to direct heating of gas decreases with increasing E/N , and is $(5-6) \cdot 10^{-2}$ at $E/N = 1.6 \cdot 10^{-16} \text{ V}\cdot\text{cm}^2$ [Ref. 45, 67]. In accordance with Ref. 71, about 5% of the total expended energy is spent on pulsed ionization of the medium, about 2% is dissipated in the ballast resistors, and 10% is lost in the layers near the electrodes. The value of $\eta_p \sim 0.80-0.85$ in the NDIP exceeds the corresponding values for the transverse self-maintained dc discharge by a factor of 1.5-2. Experiments with prolonged lasing under closed-cycle conditions have been done only for the longitudinal version of the gas-discharge chamber (see Fig. 13c), and have demonstrated the feasibility of attaining $P = 6 \text{ kW}$ at $\eta_{90} \sim 0.1$ [Ref. 72].

In comparing NDIP with other pumping methods, it must be noted that use of this technique obviates certain technical complexities that arise when NDEB is used. Specific and integrated characteristics of such lasers may be double or triple the corresponding characteristics of lasers with pumping by self-maintained dc discharge, but still they are considerably inferior to the limiting parameters of lasers with pumping by NDEB. One of the major technical complexities in making a laser with pumping by NDIP is development of a nanosecond pulse generator.

2.4. Ac discharge

One of the promising methods of pumping convective lasers is the ac discharge. The idea of using an ac discharge was first put forth in 1974 [Ref. 73], and was then intensely developed in a number of papers [Ref. 74, 78, 85, 86]. In contrast to non-self-maintained discharges, the ac discharge does not require several supply sources for realization, and it is fairly simple to realize.

The physical mechanism of such a discharge is reminiscent of the mechanism of the NDIP (Fig. 14a). Just as in the NDIP, ionization in the ac discharge takes place only as the absolute value of the electric field is passing through the maximum, rather than during the entire discharge period; for the rest of the time the discharge is non-self-maintained, and current is flowing in the decaying plasma. The frequency f of the ac discharge on the one hand must be greater than the effective frequency of plasma decay, and on the other hand must not be too high, so that the discharge in the plasma is not pinched by displacement currents, i. e. it must satisfy the condition

$$(\beta_0 n_e) \ll f \ll \sigma,$$

where σ is plasma conductivity. Substituting values of $\beta_0 n_e \sim 10^3$ and $\sigma \sim 10^7 \text{ } \Omega^{-1}$ that are typical of laser discharges, we can readily see that the quantity f must lie in a range of 10 kHz-1 MHz. The ac discharge in a laser medium has been most completely studied in the frequency range of 10-100 kHz [Ref. 74, 85, 86]. Pumping of the active medium of a laser by rf discharge with $f = 13.6 \text{ MHz}$ was considered in Ref. 73.

35
FOR OFFICIAL USE ONLY

FOR OFFICIAL USE ONLY

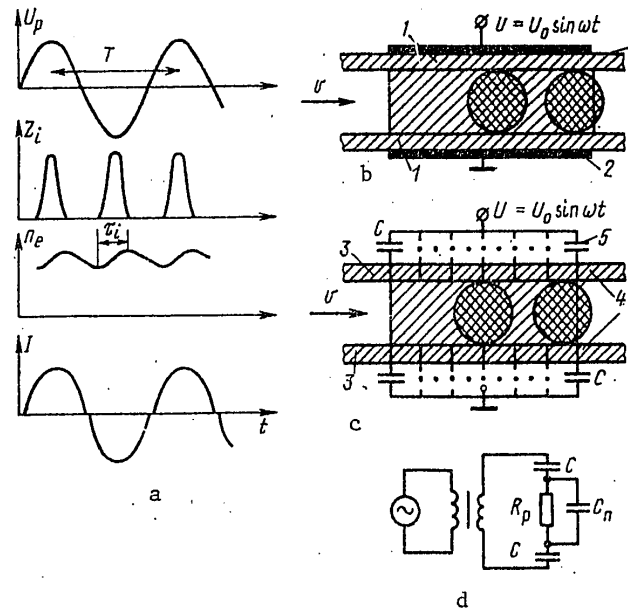


Fig. 14. Time dependences of supply source voltage U_p , laser mixture ionization rate Z_i , n_e and I (a), diagrams (b, c) and equivalent supply circuit (d) of gas-discharge chamber with ac discharge

Designs and power supply circuit of the ac gas-discharge chambers used in the experiment are shown in Fig. 14b, c. Transverse ac discharge with respect to gas flow was set up between two dielectric plates 1 with metal coatings 2 applied on the outside (electrodeless discharge) [Ref. 74], or in a chamber made up of dielectric electrode plates 3 with metal electrode pins 4 set in (electrode discharge) [Ref. 86]. In this case, the circuit of each electrode contained a ballast capacitor 5 with capacitance of $C = 50-100$ pF. Discharge supply was from a source of alternating voltage through a step-up transformer. The equivalent circuit of the ac discharge supply is shown in Fig. 14d.

The mechanism of ac discharge flow and the particulars of observed current and voltage oscillograms were discussed in Ref. 75, 77. The improved stability of the plasma in the ac discharge as compared with self-maintained dc discharge is due to a number of reasons. In the first place the phase of the self-maintained discharge that is least stable with respect to ionization-thermal instability in the ac discharge makes up only a small fraction (~ 0.1) of its period T . Secondly, the ac discharge has higher values of E/N during this phase of the discharge, and weaker dependence of the ionization coefficient on E/N . And finally, "infinite" sectionalizing of the electrode element of the discharge occurs in implementation of an ac discharge, and an increase in the degree of sectionalization is accompanied by improvement of discharge stability [Ref. 51]. The more stable character of the ac discharge enables attainment of the necessary values of jE at H increased by a factor of 1.5-2, and lengths of the pumping zone reduced by a factor of 1.5-2 as compared with the transverse version of self-maintained dc discharge (see Table 2). In this case, the values of jE may reach $5-7$ W/cm³.

36
FOR OFFICIAL USE ONLY

In contrast to non-self-maintained discharges, in the ac discharge the normalized electric field E/N varies in time, and may amount to $\sim 8 \cdot 10^{-16}$ V·cm² at the maximum. Estimates of η_K obtained by integrating its calculated values [Ref. 35, 36] with respect to the period of change in the field in the discharge yield $\eta_K \sim 0.75-0.8$, which is close to the η_K for a self-maintained dc discharge. Experimental values of the vibrational efficiency of the ac discharge on a frequency of 10 kHz at $p \sim 30-50$ mm Hg coincide with calculations. Coincidence of the efficiency of excitation of the working mixture in a self-maintained dc discharge and an ac discharge with frequency of 13.6 MHz was also pointed out in Ref. 51. If we disregard dielectric losses in the ballast capacitors, we find that the discharge efficiency at $H \sim 10$ cm and $p \sim 50$ mm Hg is $\eta_p = 0.9-0.95$, and $\eta_K \eta_p \sim 0.7-0.75$ (as compared with $\eta_p \sim 0.4-0.6$ for transverse self-maintained dc discharge and 0.75-0.8 for transverse NDIP). Experimental studies of the change in optical characteristics, in particular the weak-signal gain of the medium being pumped by an ac discharge under closed-cycle conditions have shown that the necessary rate of renewal of the mixture in lasers with ac discharge is the same as with self-maintained dc discharge. Typical parameters of gas-discharge chambers of lasers with ac discharge are shown in Table 2. A comparison of the values given in the tables shows that the ac discharge is close to the NDIP with respect to limiting characteristics.

One of the peculiarities of excitation of gas-discharge lasers by ac discharge is unavoidable modulation of emission with frequency $2f$. In the case of convective lasers, the depth of modulation, just as for diffusion lasers, does not exceed 5-10% [Ref. 31, 85] at $f = 10$ kHz, and drops with increasing f .

In discussing the technical aspects of developing laser equipment, we must note the relative simplicity of laser pumping by ac discharge. Like semi-self-maintained discharges, it can produce a homogeneous medium in large volumes with higher interelectrode gap (~ 10 cm) and comparatively short pumping zone (~ 20 cm). Such a laser can be supplied by a simple and reliable source consisting of a motor-generator and step-up transformer. Another important condition for feasibility of using an ac discharge in laser equipment is the availability of industrial motor-generator sets with frequency of 8-10 kHz and power up to 150 kW.

The ac discharge is a promising pumping method not only for convective lasers, but for diffusion lasers as well [Ref. 31]. This technique eliminates energy losses in ballast resistors, reduces the voltage of the laser supply source, and also enables electrodeless discharge, which may be of interest for sealed diffusion lasers.

Recently there have been indications of the feasibility in principle of further increasing the limiting characteristics of ac discharges by rotating the electric field vector [Ref. 79, 81]. The first reports have also appeared on experimental confirmations of improvement of discharge stability in rotating electric fields with frequency of 1 MHz [Ref. 82-83]. However, the small scale of these experiments and lack of data on the characteristics of such a discharge in a gas flow do not permit consideration of the discharge in rotating electric fields as an investigated method of pumping convective lasers.

Conclusion

The present state of gas discharge physics and engineering now enables us to make efficient laser devices with steady-state emission power up to 10 kW, and opens up

FOR OFFICIAL USE ONLY

prospects for further considerable increase of power and improvement of operational characteristics of gas-discharge process lasers.

Selection of the laser design and pumping method should be determined of course not only by the power of the laser, but also by its purpose, working conditions, and economic effectiveness of utilization.

Analysis of non-Soviet models of process lasers has shown that the cost of the laser itself as normalized to the output power is weakly dependent on the laser design and the pumping method used, and decreases from 90-110 to 20-40 dollars per watt as power increases from 1-2 to 10 kW [Ref. 8].

More important from the economic standpoint is the cost of laser operation. The efficiencies of different laser systems are similar, usually amounting to 5-10%. The cost of using CO₂ lasers is determined to a great extent by their capability for using inexpensive working mixtures, especially helium-free mixtures, since the overwhelming majority of present-day process lasers with convective cooling are operated under conditions of partial renewal of the laser mixture (~1% of the flowrate in the loop), and diffusion lasers operate under open-cycle conditions. Elimination of helium from the mixture composition leads to a sharp drop (by nearly an order of magnitude) in the output characteristics of the diffusion laser due to impairment of heat transfer to the walls. In convective lasers, the absence of helium does not have such an appreciable effect, especially in lasers with pumping by self-maintained dc and ac discharges. Development of efficient systems for regenerating the working medium will in principle enable a considerable reduction in the expenditure of helium and will reduce labor servicing expenditures; however, this involves the necessity of adhering to more rigorous requirements for gas-tightness of laser systems, and improved vacuum hygiene. Therefore the final choice of a laser design and pumping method requires careful analysis of their technical, operational and economic aspects.

REFERENCES

1. Patel, C. K. N., PHYS. REF. LETTS, Vol 13, 1964, p 617.
2. Patel, C. K. N., Faust, W. L., McFarline, R. A., BULL. AMER. PHYS. SOC., Vol 9, 1964, p 600.
3. Klauss, P. J., AVIATION WEEK AND SPACE TECHNOLOGY, Vol 103, No 9, 1975, pp 50, 103.
4. Cleo, P. K., IEEE J, Vol QE-3, 1967, p 683.
5. Tiffany, W. B., Targ, R., Foster, J. D., APPL. PHYS. LETTS, Vol 15, 1969, p 91.
6. Hoag, E., Pease, H., Staal, J., Zar, J., APPL. OPTICS, Vol 13, 1974, p 1959.
7. LASER FOCUS, Vol 13, No 3, 1977, p 14.
8. Spalding, I. J., OPTICS AND LASER TECHNOLOGY, No 1, 1978, p 29.
9. Nagai Akio, MITSUBISHI ELECTR. ADV., Vol 8, No 1, 1979, p 14.

10. Stel'makh, M. F., ed., "Lazery v tekhnologii" [Lasers in Technology], Moscow, Energiya, 1975.
11. Kosyrev, F. K., Kosyreva, N. P., Lunev, Ye. I., AVTOMATICHESKAYA SVARKA, No 9, 1976, p 72.
12. Abil'sitov, G. A., Antonova, L. I., Artamonov, A. V., Golubev, V. S., Drobyazko, S. V., Yegorov, Yu. A., Katsuro, N. I., Kazhidub, A. V., Lebedev, F. V., Senatorov, Yu. M., Sidorenko, Ye. M., Sumerin, V. V., Turundayevskiy, V. B., Frolov, V. M., KVANTOVAYA ELEKTRONIKA, Vol 6, 1979, p 204.
13. Basov, N. G., Kobayev, N. K., Danilychev, V. A., Mikhaylov, M. D., Orlov, V. K., Savel'yev, V. V., Son, V. G., Cheburkin, N. V., KVANTOVAYA ELEKTRONIKA, Vol 6, 1979, p 772.
14. Sobolev, N. N., Sokovikov, V. V., USPEKHI FIZICHESKIKH NAUK, Vol 91, 1967, p 425.
15. Tychinskiy, V. P., USPEKHI FIZICHESKIKH NAUK, Vol 91, 1967, p 389.
16. Haas, R. A., PHYS. REV., Vol 8A, 1973, p 1017.
17. Yeletskiy, A. V., Rakhimov, A. T., KHIMIYA PLAZMY, No 4, 1977, p 123.
18. Napartovich, A. P., Starostin, A. N., KHIMIYA PLAZMY, No 6, 1979, p 153.
19. Velikhov, Ye. P., Pis'mennyy, V. D., Rakhimov, A. T., USPEKHI FIZICHESKIKH NAUK, Vol 122, 1977, p 419.
20. Hertzberg, A., J. ENERGY, Vol 1, No 6, 1977, p 331.
21. J. P. Reilly, ASTRONAUTIC-AERONAUTICS, No 3, 1975, p 52.
22. Levinson, G. R. et al., ZHURNAL PRIKLADNOY SPEKTROSKOPII, Vol 10, 1969, p 425.
23. Ochkin, V. N., TRUDY FIZICHESKOGO INSTITUTA IMENI P. N. LEBEDEVA AKADEMII NAUK SSSR, Vol 78, 1974, p 3.
24. Brown, C. O., Davis, J. W., APPL. PHYS. LETTS., Vol 21, 1972, p 480.
25. Rayzer, Yu. P., FIZIKA PLAZMY, Vol 5 1979, p 408.
26. Bondarenko, A. V., Golubev, V. S., Dan'shchikov, Ye. V., Lebedev, F. V., Ryazanov, A. V., FIZIKA PLAZMY, Vol 5, 1979, p 687.
27. Ecker, G., Kroll, W., Zöllner, PHYS. FLUIDS, Vol 7, 1964, p 2001.
28. Abil'sitov, G. A., Artamonov, A. V., Velikhov, Ye. P., Yegorov, Yu. A., Kazhidub, A. V., Lebedev, F. V., Sidorenko, Ye. M., Sumerin, V. V., Frolov, V. M., KVANTOVAYA ELEKTRONIKA, Vol 7, 1980, p 2467.

FOR OFFICIAL USE ONLY

29. Locke, E., OPTICAL ENGINEERING, Vol 17, 1978, p 192.
30. French Patent No 70, 37698, 19 Oct 70.
31. Antyukhov, V. V., Glova, A. F., Kachurin, O. R., Lebedev, F. V., KVANTOVAYA ELEKTRONIKA, Vol 7, 1980, p 425.
32. Kozlov, G. I., Kuznetsov, V. A., Masyukov, V. A., PIS'MA V ZHURNAL TEKHNIЧЕСКОY FIZIKI, Vol 4, 1978, p 129.
33. Letokhov, V. S., Ustinov, N. D., "Moshchnyye lazery i ikh primeneniye" [Powerful Lasers and Their Use], Moscow, Sovetskoye radio, 1980.
34. Artamonov, A. V., Yegorov, Yu. A., Kazhidub, A. V., Katsuro, N. I., Lebedev, F. V., Sidorenko, Ye. M., Sumerin, V. V., Frolov, V. M. KVANTOVAYA ELEKTRONIKA, Vol 5, 1978, p 920.
35. Nighan, W. L., PHYS. REV., Vol A2, 1970, p 1989.
36. Karlov, N. V., Konev, Yu. B., Kochetov, I. V., Pevgov, V. G., Preprint, Lebedev Physics Institute, No 91, Moscow, 1976.
37. Granovskiy, V. D., "Elektricheskiy tok v gaze" [Electric Current in Gas], Moscow, Nauka, 1971.
38. Lancashire, R. B., Alger, D. L., Manista, E. J., Scalby, J. G., Dunnig, J. W., Stubbs, R. M., OPTICAL ENGINEERING, Vol 16, 1977, p 505.
39. Myl'nikov, G. D., Napartovich, A. P., FIZIKA PLAZMY, Vol 1, 1975, p 892.
40. Eckbreth, A. C., Davis, J. W., APPL. PHYS. LETTS, Vol 19, 1971, p 101.
41. Rayzer, Yu. P., "Osnovy sovremennoy fiziki gazorazryadnykh protsessov" [Principles of Modern Physics of Gas-Discharge Processes], Moscow, Nauka, 1980.
42. Fahlen, T. S., Kirk, R. F., U. S. Patent No 4077018, 28 Feb 78.
43. Artamonov, A. A., Blokhin, V. I., Vedenov, A. A., Vitshas, A. F., Gavriilyuk, V. D., Yegorov, A. A., Naumov, V. G., Pashkin, S. V., Peretyat'ko, P. I., KVANTOVAYA ELEKTRONIKA, Vol 4, 1977, p 581.
44. Vedenov, A. A., Vitshas, A. F., Gerts, V. Ye., Naumov, V. G., TEPILOFIZIKA VYSOKIKH TEMPERATUR, Vol 14, 1976, p 441.
45. Akishev, Yu. S., Artamonov, A. V., Naumov, V. G., Trushkin, N. I., Shashkov, V. M., ZHURNAL TEKHNIЧЕСКОY FIZIKI, Vol 49, 1979, p 900.
46. Artamonov, A. V., Breyev, V. V., Kukhareenko, A. T., Samokhin, A. A., "Trudy vtorogo Vsesoyuznogo soveshchaniya po fizicheskim protsessam v gazovykh OKG" [Proceedings of Second All-Union Convention on Physical Processes in Gas Lasers], Uzhgorod, 1978.

10
FOR OFFICIAL USE ONLY

47. Vedenov, A. A., Vitshas, A. F., Dykhne, A. M., Myl'nikov, G. D., Napartovich, A. P., "Trudy odinnadtsatoy Mezhdunarodnoy konferentsii po ionizirovannym gazam" [Proceedings of Eleventh International Conference on Ionized Gases], Prague, 1973,
48. Baranov, V. Yu., Niz'yev, V. G., Figul'skiy, S. V., FIZIKA PLAZMY, Vol 4, 1978, p 858.
48. Akishev, Yu. S., Pashkin, S. V., TEPLOFIZIKA VYSOKIKH TEMPERATUR, Vol 15, 1977, p 703.
50. Akishev, Yu. S., Pashkin, S. V., Soklov, N. A., FIZIKA PLAZMY, Vol 4, 1978, p 858 [sic].
51. Eckbreth, A. C., Davis, J. W., APPL. PHYS. LETTS, Vol 21, 1972, p 25.
52. Hill, A. E., IEEE PAPER No 71-65.
53. Gentle, K. W. et al., NATURALE, Vol 203, 1964, p 1369.
54. Garosi, G. A. et al., PHYS. FLUIDS, Vol 13, 1970, p 2795.
56. Galechan, G. R., Petrosyan, S. I., ZHURNAL PRIKLADNOY MEKHANIKI I TEKHNICHESKOY FIZIKI, No 6, 1975, p 9.
57. Eckbreth, A. C., Owen, F. S., REV. SCI. INSTR. Vol 43, 1972, p 995.
58. Weingard, W. J., Nighan, W. L., APPL. PHYS. LETTS, Vol 26, 1975, p 544.
59. Polulyakh, V. P., Kiselev, V. I., IZVESTIYA VYSSHIKH UCHEBNYKH ZAVEDENIY: SERIYA FIZIKA, No 5, 1977, p 125.
60. Generalov, N. A., Zimakov, V. P., Kosynkin, V. D., Rayzer, Yu. P., Roytenburg, D. I., FIZIKA PLAZMY, Vol 3, 1977, p 626.
61. Dan'shchikov, Ye. V., Golubev, V. S., Lebedev, F. V., "Trudy Chetvertoy konferentsii po fizike nizokotemperaturnoy plazmy" [Proceedings of Fourth Conference on Low-Temperature Plasma Physics], Kiev, 1975.
62. Rakhimov, T. V., Rakhimov, A. T., TEPLOFIZIKA VYSOKIKH TEMPERATUR, Vol 14, 1976, p 1313.
63. Rayzer, Yu. P., Shapiro, G. I., FIZIKA PLAZMY, Vol 4, 1978, p 850.
64. Basov, N. G., Belenov, E. M., Danilychev, V. A., Suchkov, A. F., USPEKHI FIZICHESKIKH NAUK, Vol 114, 1974, p 213.
65. Velikhov, Ye. P., Golubev, S. A., Kovalev, A. S., Persiantsev, I. G., Pis'mennyy, V. D., Rakhimov, A. T., Rakhimova, T. V., FIZIKA PLAZMY, Vol 1, 1975, p 847.
66. Babichev, V. N., Golubev, S. A., Kovalev, A. S., Pis'mannyy, V. D., Rakhimov, A. T., FIZIKA PLAZMY, Vol 6, 1980, p 195.

41
FOR OFFICIAL USE ONLY

FOR OFFICIAL USE ONLY

67. Artamonov, A. V., Naumov, V. G., Shachkin, L. V., Shashkov, V. M., KVANTOVAYA ELEKTRONIKA, Vol 6, 1979, p 1442.
68. Reilly, J. R., APPL. PHYS., Vol 43, 1972, p 3411.
69. Hill, H. E., APPL. PHYS. LETTS, Vol 12, 1973, p 570.
70. Napartovich, A. P., Naumov, V. G., Shashkov, V. M., FIZIKA PLAZMY, Vol 1, 1975, p 821.
71. Naumov, V. G., Shashkov, V. M., KVANTOVAYA ELEKTRONIKA, Vol 4, 1977, p 2427.
72. Generalov, N. A., Zimakov, V. P., Kosynkin, V. D., Rayzer, Yu. P., Roytenburg, D. I., PIS'MA V ZHURNAL TEKHNICHESKOY FIZIKI, Vol 1, 1975, p 431; FIZIKA PLAZMY, Vol 6, 1980, p 1152.
73. Goykhman, V. Kh., Gol'dfarb, V. M., ZHURNAL PRIKLADNOY SPEKTROSKOPII, Vol 21, 1974, p 456.
74. Gavriilyuk, V. D., Glova, A. F., Golubev, V. S., Lebedev, F. V., KVANTOVAYA ELEKTRONIKA, Vol 4, 1977, p 2034.
75. Barkalov, A. D., Gavriilyuk, V. D., Gladush, G. G., Glova, A. F., Golubev, V. S., Lebedev, F. V., TEPILOFIZIKA VYSOKIKH TEMPERATUR, Vol 16, 1978, p 265.
76. Belikov, A. V., Glova, A. F., Golubev, V. S., Lebedev, F. V., "Trudy pyatoy Vsesoyuznoy konferentsii po fizike nizokotemperaturnoy plazmy" [Proceedings of Fifth All-Union Conference on Low-Temperature Plasma Physics], Kiev, 1979.
77. Barkalov, A. D., Gladush, G. G., Glova, A. F., Golubev, V. S., Lebedev, F. V., TEPILOFIZIKA VYSOKIKH TEMPERATUR, Vol 18, 1980, p 483.
78. Glova, A. F., Golubev, V. S., Lebedev, F. V., TEPILOFIZIKA VYSOKIKH TEMPERATUR, Vol 17, 1979, p 220.
79. Shapiro, G. I., PIS'MA V ZHURNAL TEKHNICHESKOY FIZIKI, Vol 2, No 10, 1976, p 451.
80. Shapiro, G. I., PIS'MA V ZHURNAL TEKHNICHESKOY FIZIKI, Vol 4, No 7, 1978, p 393.
81. Shapiro, G. I., TEPILOFIZIKA VYSOKIKH TEMPERATUR, Vol 18, 1980, p 40.
82. Zhilinskiy, A. P., Kuteyev, B. V., Smirnov, A. S., Shevchenko, Yu. I., ZHURNAL TEKHNICHESKOY FIZIKI, Vol 48, 1978, p 2260.
83. Kuteyev, B. V., Smirnov, A. S., ZHURNAL TEKHNICHESKOY FIZIKI, Vol 49, No 8, 1979, p 1615.
84. Antyukhov, V., Bondarenko, A., Glova, A. F., Kachurin, O. R., Kolesov, L. L., Lebedev, Ye. A., Lebedev, F. V., Suslov, Yu. F., Timofeyev, V. A., KVANTOVAYA ELEKTRONIKA, Vol 8, 1981, p 2234.

42
FOR OFFICIAL USE ONLY

85. Gavriilyuk, V. D., Glova, A. F., Golubev, V. S., Kuznetsov, A. B., Lebedev, F. V., Feofilaktov, V. A., KVANTOVAYA ELEKTRONIKA, Vol 6, 1979, p 548.
86. Bondarenko, A. V., Gavriilyuk, V. D., Golubev, V. S., Lebedev, F. V., Smakotin, M. M., KVANTOVAYA ELEKTRONIKA, Vol 7, 1980, p 775.

COPYRIGHT: Izdatel'stvo "Radio i svyaz'", "Kvantovaya elektronika", 1981

6610
CSO: 1862/91

43
FOR OFFICIAL USE ONLY

FOR OFFICIAL USE ONLY

UDC 621.373.826

CHANGE IN RELAXATION RATE OF UPPER LASER LEVEL WITH PROLONGED OPERATION OF CW ELECTRON-BEAM-CONTROLLED CO₂ PROCESS LASER

Moscow KVANTOVAYA ELEKTRONIKA in Russian Vol 8, No 12(114), Dec 81 (manuscript received 5 Jun 81) pp 2710-2712

[Article by A. P. Averin, Ye. P. Glotov, V. A. Danilychev, N. N. Sazhina, A. M. Soroka and V. I. Yugov, Physics Institute imeni P. N. Lebedev, USSR Academy of Sciences, Moscow]

[Text] Experimental studies are done on the change in parameters of an electroionization discharge and lasing efficiency in the course of prolonged continuous operation of a closed-cycle CO₂ process laser with power of 10 kW. It is shown that in the process of prolonged laser operation, there is a reduction not only in discharge current, but also in lasing efficiency as a result of impurity formation in the laser mixture, increasing the rate of relaxation of the upper laser level.

One of the main factors that determine economic efficiency of laser technology is the process of degradation of the laser mixture [Ref. 1]. It is known [Ref. 2] that the principal cause of reduced energy input during operation of electroionization lasers in the pulse-periodic mode is formation of nitrogen oxides in the laser mixture under the action of the electron beam. The oxide molecules have electron sticking cross sections more than 100 times those of oxygen molecules. In pulse-periodic electroionization lasers, the pumping power is usually considerably greater than the power of relaxation losses, and the formation of relatively low concentrations of N₂O and NO₂ (10⁻²%) does not lead to any reduction of lasing efficiency within the limits of measurement error. In cw CO₂ electroionization lasers, the pumping power is commensurate with the power of relaxation losses, and therefore the presence of molecular gas impurities in the laser mixture may lead to an appreciable reduction of lasing efficiency as a result of a reduction in the time of relaxation of the upper laser level 00⁰¹.

This paper is devoted to an experimental study of the characteristics of the electroionization discharge and lasing efficiency in the course of prolonged continuous operation of a closed-cycle electroionization process laser with emission power of 10 kW shown schematically in Fig. 1a.

The laser mixture was ionized by triode electron gun 1 with thoriated tungsten cathode [Ref. 1]. The maximum working current density j_{e*} of the electron beam

111
FOR OFFICIAL USE ONLY

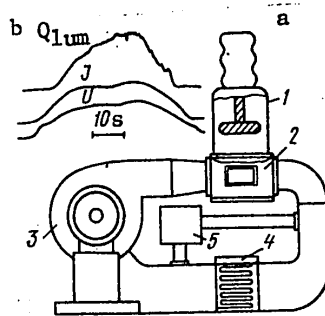


Fig. 1. Diagram of electroionization laser (a) and typical loop oscillogram of voltage U ($U_{max} = 2.5$ kV), discharge current I ($I_{max} = 45$ A) and lasing power Q_{lum} ($Q_{max} = 10$ kW) at electron beam current density $j_e = 12 \mu A/cm^2$ and pressure of the laser mixture $CO_2:N_2:He = 1:30:29$ of $p = 50$ mm Hg (b)

in the cathode plane of the discharge chamber 2 as determined by superheating of the separative foil of the electron gun was $12 \mu A/cm^2$. Blower 3 provided a circulating rate of the laser mixture at the input to the discharge chamber of up to 90 m/s. The laser mixture was cooled in tubular heat exchanger 4, keeping the gas temperature at the input to the active volume at 320 K.

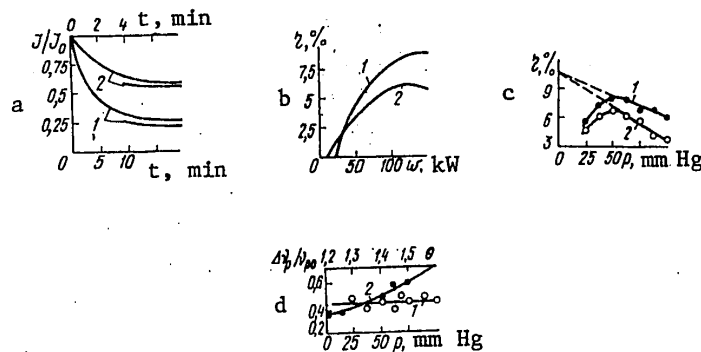


Fig. 2. Ratio of discharge current I to discharge current I_0 in a "fresh" mixture (a) as a function of time of continuous laser operation without regenerator (1) and with regenerator (2); lasing efficiency η as a function of pumping power (b) for a "fresh" mixture (1) and for a mixture with 2-minute depletion (2) at $p = 50$ mm Hg; lasing efficiency as a function of pressure of the laser mixture (c) at constant normalized pumping power $w/p = 1.5$ kW/mm Hg (gas flowrate 9 m³/s) for "fresh" (1) and "stale" (2) mixtures; relative increase in rate of relaxation losses as a function of pressure (1) and average adjusted temperature of the laser mixture $\theta = T_{av}/300$ K (2) (d)

45
FOR OFFICIAL USE ONLY

FOR OFFICIAL USE ONLY

To determine the way that discharge current and lasing efficiency depend on the working time of the electroionization laser, current-photovoltage characteristics were taken at different instants. A typical loop oscillogram of these characteristics is shown in Fig. 1b. To eliminate the possibility of additional accumulation of nitrogen oxides that might occur in breakdowns of the discharge gap, the working voltage in taking the current-photovoltage characteristics was not raised to the threshold value (E/p) corresponding to discharge contraction. Fig. 2a shows curves for the discharge current density as a function of continuous laser operation time without regeneration of the laser mixture (curve 1) and with the use of a regenerator (2) [Ref. 1]. It can be seen that when catalytic regenerator 5 (Fig. 1) is used, the rate of degradation of the laser mixture is considerably reduced, but the discharge current cannot be totally recovered.

Fig. 2b shows curves for lasing efficiency as a function of pumping power for a cw CO₂ electroionization laser with "fresh" and "stale" (2-minute depletion) mixtures of CO₂:N₂:He = 1:30:29. At first, with low pumping powers corresponding to low field strengths, the lasing efficiency on the "fresh" mixture is lower. This is due to the fact that in the first case the same pumping power $w = jE$ is realized at a lower normalized field strength $(E/p)_1 = (E/p)_2 j_2 / j_1 \approx 0.75 \cdot (E/p)_2$, and accordingly at considerably lower efficiency of excitation of the upper laser level and vibrational levels of nitrogen η_{ef} whose value at low E/p rises sharply as the normalized field strength is increased [Ref. 3]. At high pumping powers corresponding to the range of working parameters of the cw CO₂ electroionization laser, curve 2 is situated lower than curve 1. This is due to the increase in relaxation rate of the upper laser level ν_p as nitrogen oxides accumulate in the electroionization discharge.

To determine the way that the change in relaxation rate during degradation of the laser mixture depends on excitation parameters, let us consider expressions for lasing efficiency [Ref. 4] of a "fresh" (1) and "stale" (2) laser mixture with constant energy input per unit of mass of the circulating gas:

$$\eta_0 = \eta_{KB} \eta_p \eta_d \eta_{ef} \eta_W - \eta_{KB} \eta_p Q_{*a}(w) \rho / w_a, \quad (1)$$

$$\eta_1 = \eta_{KB} \eta_p \eta_d \eta_{ef} \eta_W - \eta_{KB} \eta_p Q_{*a}(w) \nu_{p1} \rho / (w_a \nu_{p0}), \quad (2)$$

where η_{KB} and η_p are quantum efficiency and resonator efficiency; η_d is the efficiency of the discharge determined by electrode potential drops $U_{AK} (\eta_d = 1 - U_{AK}/U_0)$; $\eta_W = 1 - W_* \dot{m}/w$, W_* is the threshold pumping energy at the end of the active volume, i. e. the energy carried off by the flow from the discharge chamber; $w_a = w/p$ is the normalized pumping power; $\dot{m}_a = \dot{m}/p$ is the normalized gas flowrate; $Q_{*a}(w) = Q_*(w)/p^2$ is the normalized power of relaxation losses. At high field strengths, the excitation efficiency η_{ef} and discharge efficiency η_d are weakly dependent on E/p , and the relation between the change in lasing efficiency and the change in relaxation rate $\Delta \nu_p$ is written as

$$\Delta \eta = \eta_p \eta_{KB} Q_{*a}(w_a) \rho \Delta \nu_p / (w_a \nu_{p0}), \quad (3)$$

where the dimensionless coefficient $\eta_{KB} \eta_p Q_{*a} p / w_a$ is determined from the dependence of efficiency on pressure shown in Fig. 2c. At low pressures, η increases with p . This is due to the reduction in the fraction of energy carried off from the active volume by the gas flow as a result of an increase in the rate of excitation transfer

from N_2 to CO_2 , as well as to the increase in η_d caused by a reduction in the relative cathodic potential drop U_{ak}/U_0 as pressure rises [Ref. 5]. At high pressures, the pressure dependence of η_d and η_w ceases, and lasing efficiency with increasing p falls off linearly due to the increasing rate of relaxation losses. Experimental points fit well on a straight line (see Fig. 2c) for which the tangent of the slope is

$$\text{tg}\alpha = \eta_p \eta_{KB} \eta_{ef} \eta_d \eta_w / w_a.$$

The product $\eta_{KB} \eta_p \eta_{ef} \eta_d \eta_w$ is determined by the point where this line extended intersects the axis of ordinates.

Fig. 2d shows the pressure dependence of relative increase in rate of relaxation losses for a gas mixture after two minutes of depletion. It can be seen that the quantity $\Delta v_p / v_{p_0}$ determined in this way does not depend on pressure within the limits of measurement error, and not only on the linear section of curve $\eta(p)$, but at low p as well. The scatter of the experimental points enables us to estimate the relative error of measurements $\delta(\Delta v/v)$ by the proposed technique, which in the given case does not exceed 10-15% (see Fig. 2c). Determining $\Delta v_p / v_{p_0}$ similarly for other values of specific energy input, we can plot the curve for the relative increase in relaxation rate of the upper laser level as a function of average gas temperature $2T_{av} = T_0 [1 + w / (C_p T_0 m)]$ (see Fig. 2d). It is evident that the quantity $\Delta v_p / v_{p_0}$ increases with rising average gas temperature, i. e. the rate of relaxation of excited CO_2 molecules by nitrogen oxide impurities is a stronger function of temperature than for the main components of the laser mixture. This is indirect confirmation of the following mechanism of relaxation by impurities: resonant transfer of excitation from the asymmetric level of CO_2 to the vibrational level of nitrogen oxides (most probably N_2O) and subsequent transfer to heat, which is the limiting factor for the entire process.

REFERENCES

1. Basov, N. G., Babayev, I. K., Danilychev, V. A. et al., KVANTOVAYA ELEKTRONIKA, Vol 6, 1979, p 772.
2. Glotov, Ye. P., Danilychev, V. A., Zvorykin, V. D. et al., KVANTOVAYA ELEKTRONIKA, Vol 7, 1980, p 630.
3. Lobanov, A. N., Orlov, V. K., Suchkov, A. F., Urin, B. M., Preprint, Lebedev Physics Institute, No 199, Moscow, 1977.
4. Basov, N. G., Glotov, Ye. P., Danilychev, V. A., Soroka, A. M., KVANTOVAYA ELEKTRONIKA, Vol 7, 1980, p 1067.
5. Aleksandrov, V. V., Koterov, V. N., Soroka, A. M., ZHURNAL VYCHISLITEL'NOY MATEMATIKI I MATEMATICHESKOY FIZIKI, Vol 18, 1978, p 1214.

COPYRIGHT: Izdatel'stvo "Radio i svyaz'", "Kvantovaya elektronika", 1981

6610
CSO: 1862/91

47
FOR OFFICIAL USE ONLY

FOR OFFICIAL USE ONLY

OPTICS AND SPECTROSCOPY

UDC 621.373.826

HOLOGRAPHIC MEASUREMENTS

Moscow GOLOGRAFICHESKIYE IZMERENIYA in Russian 1981 (signed to press 3 Aug 81)
pp 2-5, 295-296

[Annotation, foreword and table of contents from book "Holographic Measurements",
by Vera Moiseyevna Ginzburg and Boris Mikhaylovich Stepanov, Izdatel'stvo
"Radio i svyaz'", 8000 copies, 296 pages]

[Text] The theoretical fundamentals of holographometry are discussed, a description is given of a holographic measuring complex of apparatus making it possible to record holograms and interferograms of stationary and dynamic entities, and algorithms for processing holographic information for obtaining quantitative measurement data are presented.

For engineering and technical personnel using holographic measuring methods in their work.

Foreword

Holography is a new trend in applied physics which appeared relatively recently but has gained a wide reputation among specialists in various fields and even among the general public.

The popularity of holography is the result of its enticing possibilities, making it possible to expand considerably the limits of man's knowledge of his natural environment, to create completely new graphic equipment and new more informative computers and recognition systems, and to accomplish nondestructive testing and make precise measurements of products in the production process, including where previously for these purposes only quantitative methods of evaluation were used or measurements and testing were impossible.

After the appearance in print of the works of the founders of holography the number of publications has grown from year to year. Monographs and review books have been published in which the fundamentals of holography are discussed and examples are given of its application. In these publications and numerous articles questions relating to the application of holography as a new method of measuring and the metrological problems involved in this have practically not been elucidated, such as the requirements for holographic measuring equipment, the

48
FOR OFFICIAL USE ONLY

development of this equipment and of procedures for the main kinds of measurements, the conditions for obtaining unambiguous and reliable measurement results, etc.

The question of the use of methods of holography in metrology and of the development of measurements as a division of metrology was posed by the authors for the first time in 1971 and has been partly reflected in monographs.

At the present time holographic measurements (or holographometry) represent a relatively young rapidly growing division of the science of the measurement of processes and physical quantities, uniting a combination of methods and facilities utilizing all kinds of measurements employed in holographic methods for the purpose of extracting complete and reliable quantitative information on a three-dimensional entity or process from a hologram on which is recorded the interference pattern between a diffracted wave coming from the entity or process and a homogeneous coherent background.

This book, devoted to the physical fundamentals of holographometry, is based mainly on original work by the authors and their students performed in 1967-1980.

The book has five chapters. In the first the objectives of practical holography as a new kind of measurement of processes and quantities are discussed, the key systems and methods used for measuring are described, general requirements for the structure of a holographic measuring complex and the objectives of metrological provision for holographic measurements are formulated, and the key specifications of facilities for testing holographic measuring equipment are discussed. A description is given of holographic measuring equipment series-produced in the USSR for recording holograms in the optical waveband; concise information is given on new holographic devices and apparatus in the development stage.

In the second chapter the physical fundamentals of methods of holographic measurement and their key metrological characteristics are discussed, and the results are given of an analysis of the key elements of the holographic process from the viewpoint of determining sources of errors and substantiating requirements imposed on radiation sources and holographic systems and equipment designed for making holographic measurements of stationary and dynamic entities. Theoretical and practical aspects of the implementation of methods of holographic measurement in the optical and microwave bands are discussed.

In the third chapter methods of processing holographic information are described: photogrammetric, machine and correlation. New methods of isolating the distinctive features of an image are discussed, based on the use of certain data on the recognition of patterns by man, making it possible to construct optimized correlation systems of recognition. A brief description is given of multichannel holographic correlators ready for series production. A description is given of algorithms for the digital processing of holographic interferograms, the digital reconstruction of holograms obtained in the non-optical band, and the digital simulation of holographic processes and systems.

49
FOR OFFICIAL USE ONLY

FOR OFFICIAL USE ONLY

In the fourth and fifth chapters applications of methods and equipment for holographic measurement for solving national economic problems are elucidated, including nondestructive control of the quality of optical waves; studies of processes in living cells; nondestructive control of the quality of crystals, including in the process of their growth; studying the process of the combustion of condensed matter; determining the continuity of multicomponent flows; studying the process of the fuel supply in diesels; determining optimum conditions for the storage of a monumental painting, etc.

All figures whose numbers are marked with asterisks are placed in the insertion at the end of the book.

The authors hope that the book will prove helpful to a wide range of readers, including developers of methods and equipment for holography, scientific personnel, engineers, biologists, physicians and restorers working in the field of holography and its applications.

The authors are deeply grateful to the reviewers of the book, USSR Academy of Sciences Corresponding Member L.D. Bakhrakh and Doctor of Physical and Mathematical Sciences Professor Yu.A. Bykovskiy, for their valuable hints, which were taken into account in revising the manuscript.

The authors wish to express their heartfelt thanks to Ya.A. Gabelev for his great help in preparing and editing the manuscript.

CONTENTS	Page
Foreword	3
Chapter 1. Holography as a Method of Measuring	
1.1. Kinds of holographic measurements and their features	6
1.2. Key methods and areas of application of holographic measurements	10
1.3. General requirements for the structure of a holographic measuring complex	15
1.4. Holographic measuring equipment	19
1.5. Metrological problems in providing for holographic measurements	36
Chapter 2. Physical Fundamentals of Methods of Holographic Measurement	
2.1. Relationship between visibility factor and parameters of interacting interference waves	41
2.2. Limitations imposed on holographic measurements of dynamic entities by the Doppler effect and ways of overcoming them	55
2.3. Holographic interference measurements of phase entities and their features	58
2.4. Holographic measurements of the dispersed phase of multicomponent dynamic systems	70
2.5. Holographic interference measurements of reflecting objects	73
2.6. Methods of holographic measurement in the microwave band	90
Chapter 3. Methods of Processing Holographic Information	
3.1. Photogrammetric methods of measuring holographic images	120
3.2. Solution to the inverse problem of determining the distribution of the refractive index of phase entities from measuring the optical path length or its derivative	126

3.3.	Holographic correlation methods of measuring	138
3.4.	Processing optical images in the input and output of holographic correlators, computers and communication channels	154
3.5.	Defocusing as a means of isolating informative fragments and the visual analyzer	158
3.6.	Defocusing as a means of producing a generalized pattern of an image in the input of a holographic correlator	166
3.7.	Representation of optical images in holographic correlators by means of genetic functions	171
3.8.	Human-like "drawing" robot	177
3.9.	Use of defocusing for automating the process of inputting holographic images into a computer	182
3.10.	Use of defocusing for narrowing the transmission band of TV channels	184
3.11.	Comparison of the defocusing method with other human-like methods of pattern recognition	185
3.12.	Digital holography	189
Chapter 4. Use of Holographic Methods of Measuring for Studying Stationary Objects and Slowly Occurring Processes		
4.1.	Study of plant cells	213
4.2.	Study of blood cells	215
4.3.	Study of crystals	221
4.4.	Nondestructive testing of optical fibers	230
4.5.	Measurement of the thickness of thin films	236
4.6.	Determination of optimum temperature and humidity conditions for storing frescoes	
4.7.	Measurement of the relief of the surface of magnetic disks	241
4.8.	Holographic nondestructive testing of products in the microwave band	244
Chapter 5. Applications of Holographic Methods of Measuring for Studying Dynamic Objects and Rapidly Occurring Processes		
5.1.	Measuring the continuity of two-phase flows	248
5.2.	Measuring distribution of velocities in a falling sheet of water	250
5.3.	Studying the process of combustion of condensed systems	253
5.4.	Studying fuses	258
5.5.	Studying discharge in flash lamps	265
5.6.	Studying the structure of dispersed annular flows	267
5.7.	Studying the fuel line of automotive diesel engines	269
5.8.	Visualization of ultrasonic fields in optically transparent media	279
	Bibliography	282
	Subject Index	291

COPYRIGHT: Izdatel'stvo "Radio i svyaz", 1981

8831

CSO: 1862/106

FOR OFFICIAL USE ONLY

UDC 535.3

FEASIBILITY OF CONTROLLING GAIN OF ENTHALPY-STIMULATED LIGHT SCATTERING

Moscow KVANTOVAYA ELEKTRONIKA in Russian Vol 8, No 12(114), Dec 81 (manuscript received 6 May 81) pp 2699-2702

[Article by V. S. Zuyev, O. Yu. Nosach and Ye. P. Orlov, Physics Institute imeni P. N. Lebedev, USSR Academy of Sciences, Moscow]

[Text] An investigation is made of the influence that laser parameters have on the gain of enthalpy-stimulated light scattering by ultrasound in the active medium of iodine photodissociation lasers. It is shown that there is a range of intensities of stimulating laser radiation in which there is a sharp drop in the gain of stimulated scattering with increasing intensity. By varying the cross section of the laser transition, this range can be shifted, and the gain of stimulated scattering can be varied over wide limits. The results are hopeful from the standpoint of getting high directionality of powerful laser emission.

It was shown in Ref. 1 that in thermodynamically nonequilibrium media in which the rates of internal processes taking place with release or absorption of energy depend on electromagnetic field intensity, a new kind of stimulated light scattering may arise. Specifically, this stimulated scattering has been considered in the active medium of iodine photodissociation lasers: $n\text{-C}_3\text{F}_7\text{I}$ vapor (0.01-0.05 atm) and buffer gases such as SF_6 or CO_2 at pressure close to atmospheric. During pumping in the active region of the photodissociation laser, as a result of photolysis, $n\text{-C}_3\text{F}_7$ radicals and excited iodine atoms I^* are formed that make the transition to the ground state under the action of resonant laser emission ($\lambda = 1.315 \mu\text{m}$). Iodine atoms in the ground state I are chemically more active and therefore the rate of energy release during the exothermal recombination reaction $n\text{-C}_3\text{F}_7 + \text{I} \rightarrow n\text{-C}_3\text{F}_7\text{I}$ is dependent on the intensity of laser radiation.

During development of this kind of stimulated scattering, various partial oscillations of the medium may be excited. For example in Ref. 1 an examination was made of stimulated scattering by ultrasound, and in Ref. 2, scattering by temperature waves was considered. Since excitation of partial oscillations of the medium is mainly at the expense of enthalpy of the thermodynamically nonequilibrium medium we suggest that this kind of stimulated scattering might be called enthalpy-stimulated light scattering.

52

FOR OFFICIAL USE ONLY

In Ref. 1, in considering enthalpy-stimulated scattering by ultrasonic waves it was assumed that the frequency of ultrasound may be greater than the probability with which iodine atoms and radicals enter into reactions, and much greater than the probability of induced transitions.

In this paper, the limitation on the probability of induced transitions used in Ref. 1 is removed, enabling analysis of the influence that the intensity of the exciting laser radiation and the cross section of the laser transition have on the gain of enthalpy-stimulated scattering by ultrasonic waves.

We will carry out this analysis assuming only that the frequency of ultrasound is much greater than the probability with which iodine atoms and radicals enter into chemical reactions. In iodine photodissociation lasers this condition is nearly always satisfied [Ref. 1]. In this connection, as implied by Ref. 1, of all the chemical reactions that occur in the active region of these lasers [Ref. 3] it is sufficient to consider only the reaction $R+I \rightarrow RI$, where R are $n\text{-C}_3\text{F}_7$ radicals for describing enthalpy-stimulated scattering by ultrasonic waves. Then the rate of energy release in a unit of volume $Q = q_1 \mathcal{K}_1 [R] [I]$, where q_1 is the energy released in one act of recombination, \mathcal{K}_1 is the rate constant of the reaction, [R] and [I] are the concentrations of radicals and unexcited iodine atoms respectively, the amplitude of oscillations of [R] in enthalpy-stimulated scattering by ultrasonic waves being much less than the amplitude of oscillations of [I].

The linearized equation of hydrodynamics with consideration of energy release Q [Ref. 4] in our case takes the form

$$\frac{\partial^2 \rho}{\partial t^2} - v_{3B}^2 \nabla^2 \rho - \Gamma \frac{\partial}{\partial t} \nabla^2 \rho = \frac{1}{T} \left(\frac{\partial \rho}{\partial S} \right)_p q_1 \mathcal{K}_1 [R] \nabla^2 \int [J] dt, \quad (1)$$

where ρ is the density of the substance, v_{3B} is the speed of sound, the term with Γ describes absorption of sound, T is absolute temperature, S is entropy.

The quantity [I] as a function of electromagnetic field intensity can be found from kinetic equations for [I] and the concentration of excited iodine atoms [I*]:

$$\frac{\partial [J]}{\partial t} = \sigma_y \left([J^*] - \frac{g_2}{g_1} [J] \right) \frac{cnE^2}{4\pi\hbar\omega_L} - \mathcal{K}_1 [R] [J], \quad (2)$$

$$\frac{\partial [J^*]}{\partial t} = w [N] - \sigma_y \left([J^*] - \frac{g_2}{g_1} [J] \right) \frac{cnE^2}{4\pi\hbar\omega_L}, \quad (3)$$

where w is the probability of photodissociation of $n\text{-C}_3\text{F}_7\text{I}$ molecules, [N] is their concentration, σ_y is the cross section of the laser transition, n is the index of refraction of the medium, $\hbar\omega_L$ is the energy of a laser field quantum, \vec{E} is the overall field of the exciting \vec{E}_L and scattered \vec{E}_S waves.

Let us consider the stationary problem. Let the fields $E_L = 1/2 e_L \{ E_L \exp(i\omega_L t - ik_L r) + \text{comp. conj.} \}$, $E_S = 1/2 e_S \{ E_S \exp(i\omega_S t - ik_S r) + \text{comp. conj.} \}$ be linearly polarized plane waves, where $|E_S|^2 \ll |E_L|^2$. In this case, the deviations of concentrations of excited and unexcited iodine atoms $[I^*]_1$ and [I] from their values $[I^*]_0$ and $[I]_0$ in the absence of stimulated scattering are small. Representing them in the form $[J^*]_1 = 1/2 [J^*] \exp(i\Omega t - iqr) + \text{comp. conj.}$ and $[J]_1 = 1/2 [J] \exp(i\Omega t - iqr) + \text{comp. conj.}$, where

FOR OFFICIAL USE ONLY

$\Omega = \omega_L - \omega_S, q = k_L - k_S$. with the aid of (2) and (3) we get a system of equations for $[\tilde{I}]$ and $[\tilde{I}^*]$ which within the framework of the above-mentioned condition takes the form

$$\frac{g_2}{g_1} \sigma_y \frac{cn|E_L|^2}{8\pi\hbar\omega_L} [\tilde{J}] - \left(\sigma_y \frac{cn|E_L|^2}{8\pi\hbar\omega_L} + i\Omega \right) [\tilde{J}^*] = \sigma_y \Delta_0 \frac{cnE_L E_S^*}{4\pi\hbar\omega_L}, \quad (4)$$

$$\left(\frac{g_2}{g_1} \sigma_y \frac{cn|E_L|^2}{8\pi\hbar\omega_L} + i\Omega \right) [\tilde{J}] - \sigma_y \frac{cn|E_L|^2}{8\pi\hbar\omega_L} [\tilde{J}^*] = \sigma_y \Delta_0 \frac{cnE_L E_S^*}{4\pi\hbar\omega_L}, \quad (5)$$

where $\Delta_0 = [J^*]_0 - \frac{g_2}{g_1} [J]_0$ and for the sake of simplicity we have set $e_L \equiv e_S$. From this we find $[\tilde{I}]$ as a function of E_L and E_S :

$$[\tilde{J}] = \frac{\sigma_y \Delta_0 cn E_L E_S^* / 4\pi\hbar\omega_L}{i\Omega + (1 + g_2/g_1) \sigma_y cn |E_L|^2 / 8\pi\hbar\omega_L}. \quad (6)$$

Substituting $[J] = [J]_0 + 1/2([\tilde{J}] \exp(i\Omega t - iqr) + \text{comp. conj.})$ with consideration of (5) in (1) and representing ρ in the form $\rho_0 + 1/2 \tilde{\rho} \exp(i\Omega t - iqr) + \text{comp. conj.}$, we find $\tilde{\rho}$. Then, using the shortened equation for E_S

$$\frac{\partial E_S}{\partial t} = -i \frac{k_S}{4e} \left(\frac{\partial e}{\partial \rho} \right)_S \tilde{\rho}^* E_L, \quad (7)$$

(ζ is read out along direction k_S ; $\epsilon = n^2$ is permittivity), and the thermodynamic relations

$$\left(\frac{\partial e}{\partial \rho} \right)_S \approx \left(\frac{\partial \rho}{\partial T} \right)_p^{-1} \left(\frac{\partial e}{\partial T} \right)_p, \quad \frac{1}{T} \left(\frac{\partial \rho}{\partial S} \right)_p = - \frac{v_{3B}^2}{\rho c_p} \left(\frac{\partial \rho}{\partial T} \right)_p$$

(c_p is specific heat), we represent the dependence of $|E_S|^2$ on ζ in the form

$$|E_S(\zeta)|^2 = |E_S(\zeta=0)|^2 \exp(g(\Omega)\zeta),$$

where

$$g(\Omega) = - \frac{|k_S|}{e} \left(\frac{\partial e}{\partial T} \right)_p \frac{q_1 \chi_1 [R] \sigma_y \Delta_0}{\rho c_p} \Omega_{MB}^2 \times \\ \times \frac{\Omega^2 \Gamma q^2 + (1 + g_2/g_1) \sigma_y I_L (\Omega^2 - \Omega_{MB}^2)}{\Omega [\Omega^2 + (1 + g_2/g_1)^2 (\sigma_y I_L)^2] [(\Omega^2 - \Omega_{MB}^2)^2 + \Omega^2 (\Gamma q^2)^2]} I_L; \quad (8)$$

$\Omega_{MB} = v_{3B}|q|$; $I_L = cn|E_L|^2 / (8\pi\hbar\omega_L)$ is the intensity of the stimulating radiation in quanta/(cm²·s). This formula is considerably simplified if we consider that the half-width of thermal Mandelstam-Brillouin scattering $2\delta\Omega_{MB} = \Gamma q^2$ [Ref. 5] is much less than Ω_{MB} . Then

$$g(\Omega) \approx \mp \frac{k_S}{2e} \left(\frac{\partial e}{\partial T} \right)_p \frac{q_1 \chi_1 [R] \Delta_0}{\rho c_p} \frac{\sigma_y I_L / \Omega_{MB}}{1 + ((1 + g_2/g_1) \sigma_y I_L / \Omega_{MB})^2} \times \\ \times \frac{\delta\Omega_{MB} \pm (1 + g_2/g_1) (\sigma_y I_L / \Omega_{MB}) (\Omega \mp \Omega_{MB})}{(\Omega \mp \Omega_{MB})^2 + (\delta\Omega_{MB})^2}. \quad (9)$$

Here and below, the upper sign corresponds to the case $\Omega > 0$, and the lower--to $\Omega < 0$. If $\sigma_y I_L / \Omega_{MB} \ll 1$, then (9) is transformed to the relation found in Ref. 1.

From (9) we can see that amplification is realized on both Stokes and anti-Stokes frequencies. The maximum $g(\Omega)$ are reached at

$$\Omega = \pm \Omega_{MB} \pm \delta \Omega_{MB} \left(\sqrt{1 + ((1 + g_2/g_1) \sigma_y I_L / \Omega_{MB})^2} \mp 1 \right) / ((1 + g_2/g_1) \sigma_y I_L / \Omega_{MB})$$

and are equal to

$$g = -\frac{k_S}{2e} \left(\frac{\partial e}{\partial T} \right)_p \frac{q_1 \chi_1 [R] \Delta_0}{\rho c_p} \frac{1}{2\delta \Omega_{MB}} \times \frac{\sigma_y I_L / \Omega_{MB}}{\sqrt{1 + ((1 + g_2/g_1) \sigma_y I_L / \Omega_{MB})^2} \mp 1} \frac{(1 + g_2/g_1) \sigma_y I_L / \Omega_{MB}}{1 + ((1 + g_2/g_1) \sigma_y I_L / \Omega_{MB})^2} \quad (10)$$

From (10) we see that g reaches a higher value on the Stokes than on the anti-Stokes frequency.

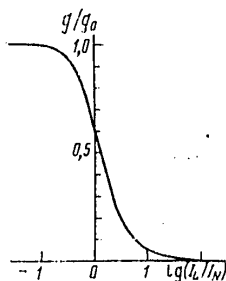
Let us consider the case of strong saturation of the laser transition, i. e. $I_L \gg I_H = ((1 + g_2/g_1) \sigma_y \tau_p)^{-1}$, where τ_p is the time of non-radiative relaxation. Here $\sigma_y I_L \Delta_0 \approx w[N]$ and g on the Stokes frequency can be represented as

$$g = \frac{1}{2} g_0 \frac{1}{\sqrt{1 + (I_L/I_N)^2} - 1} \frac{(I_L/I_N)^2}{1 + (I_L/I_N)^2} \quad (11)$$

where

$$g_0 = -k_S \left(\frac{\partial e}{\partial T} \right)_p \frac{q_1 \chi_1 [R] w [N]}{\rho c_p 2\delta \Omega_{MB} \Omega_{MB}} ; \quad I_N = \frac{\Omega_{MB}}{(1 + g_2/g_1) \sigma_y}$$

If $\sigma_y I_L \gg w$, then $[R]$, $[N]$ and consequently g_0 are practically independent of I_L [Ref. 2, 3]. Then the graph on the figure for g/g_0 as a function of I_L/I_N in essence enables us to find g as a function of I_L at different values of σ_y . Let us emphasize once more that the figure shows the region $I_L \gg I_H$. To complete the picture, let us note that if $I_L \ll I_H$, then g is proportional to I_L , i. e. $g \rightarrow 0$ if $I_L \rightarrow 0$ [Ref. 1]. The intermediate case $I_L \approx I_H$ requires separate consideration.



It is evident from the figure that g does not depend on I_L as long as $I_L/I_N \ll 1$. The conditions $I_L \gg I_H$ and $\sigma_y I_L \gg w$ do not contradict the condition $I_L/I_N \ll 1$ since the characteristic values $w \approx 10^4 \text{ s}^{-1} \ll \Omega_{MB} \approx 10^6 - 10^7 \text{ rad/s}$ [Ref. 1, 3, 6]. However, when I_L becomes much greater than I_N , g decreases as $1/I_L$. This leads to an increase in the threshold of enthalpy-stimulated scattering by ultrasonic waves, which agrees with the experimental data of Ref. 7, in which the intensity of small-scale optical inhomogeneities in the active region of the laser was attenuated as the reflectivity of the output mirror of the optical cavity was increased, i. e. with an increase in I_L . The threshold should also be exceeded with a reduction in the pressure of buffer gases, since in the first place this increases attenuation of sound, and secondly it increases σ_y [Ref. 3], leading to a reduction of $I_N \propto 1/\sigma_y$, and σ_y can be varied over a wide

FOR OFFICIAL USE ONLY

range. Apparently this explains the fact that (as far as we know) no small-scale optical inhomogeneities have been observed to arise in photodissociation lasers with pure $n\text{-C}_3\text{F}_7\text{I}$ without buffer gases.

The results demonstrate how we can influence the gain of enthalpy-stimulated scattering by ultrasonic waves, and are encouraging from the standpoint of getting high radiation intensity from powerful lasers since arising of small-scale optical inhomogeneities is quite detrimental to directionality of laser emission [Ref. 7].

These results are also applicable in the case where the assumption about the frequency of ultrasound made in our analysis is not valid. However, this case is more complicated in a mathematical sense, and requires separate consideration.

Let us note that the conclusions of this paper will apply to lasers of other types as well where the processes of energy release in the active region depend on the intensity of the laser field.

REFERENCES

1. Basov, N. G., Zuyev, V. S., Nosach, O. Yu., Orlov, Ye. P., KVANTOVAYA ELEKTRONIKA, Vol 7, 1980, p 2614.
2. Zuyev, V. S., Orlov, Ye. P., Preprint, Lebedev Physics Institute, No 145, Moscow, 1981; KVANTOVAYA ELEKTRONIKA, Vol 8, 1981, p 1968.
3. Borovich, B. L., Zuyev, V. S., Katulin, V. A., Mikheyev, L. D., Nikolayev, F. A., Nosach, O. Yu., Rozanov, V. B., "Itogi nauki i tekhniki. Seriya radio-tekhnika" [Advances in Science and Engineering. Electronics Series], Moscow, published by All-Union Institute of Scientific and Technical Information, Vol 15, 1978, pp 153-177.
4. Zel'dovich, B. Ya., Sobel'man, I. I., USPEKHI FIZICHESKIKH NAUK, Vol 101, 1970, p 3.
5. Landau, L. D., Lifshits, Ye. M., "Elektrodinamika sploshnykh sred" [Fluid Electrodynamics], Moscow, GIFML, 1959, p 501.
6. Zuyev, V. S., Katulin, V. A., Nosach, V. Yu., Petrov, A. L., TRUDY FIZICHESKOGO INSTITUT IMENI P. N. LEBEDEVA AKADEMII NAUK SSSR, Vol 125, 1980, p 46.
7. Zuyev, V. S., Netemin, V. N., Nosach, O. Yu., KVANTOVAYA ELEKTRONIKA, Vol 6, 1979, p 875.

COPYRIGHT: Izdatel'stvo "Radio i svyaz'", "Kvantovaya elektronika", 1981

6610

CSO: 1862/91

UDC 621.378.325

CONVERSION OF OPTICAL RADIATION SPATIAL SPECTRUM IN PARAMETRIC PROCESSES

Moscow KVANTOVAYA ELEKTRONIKA in Russian Vol 8, No 12(114), Dec 81 (manuscript received 15 Jan 81) pp 2690-2693

[Article by R. A. Yeremeyeva, V. A. Kudryashov, I. N. Matveyev and N. D. Ustinov]

[Text] An investigation is made of transformation of the spatial spectrum of optical emission upon passage through a stimulated nonlinear medium. The paper gives the results of experiments that confirm re-radiation by the excited nonlinear medium of energy of the plane wave of the initial radiation under certain conditions on spatial side frequencies whose spectrum corresponds to the autocorrelation function of the spatial spectrum of pumping. Two models of parametric processes are given that explain the observed effect. It is demonstrated that this phenomenon can be used for observing spatially modulated radiation propagating through a phase-distorting medium.

When optical emission passes through a nonlinear medium, some physical effects are observed that are associated with a change in the spectral makeup of the emission (generation of harmonics, sum and difference frequencies, stimulated Raman scattering, parametric luminescence and so on). Most of these effects are due to conversion of the frequency spectrum of the optical radiation; however, as the authors pointed out in Ref. 1, as a result of parametric processes we can also observe conversion of the spatial spectrum, which was later confirmed experimentally in Ref. 2, 3.

Fig. 1. Diagram of experiment: 1, 2--lenses with focal lengths f_1, f_2 ; 3--nonlinear KDP element; 4--filter of emission on frequency ω_1 ; 5--transparency; 6--focal plane of lens 1

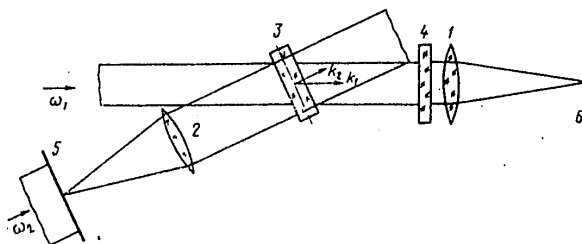


Fig. 1 shows a diagram of the experimental setup used to record the effect of transformation of only the spatial spectrum of optical radiation while retaining

57
FOR OFFICIAL USE ONLY

FOR OFFICIAL USE ONLY

the frequency spectrum unchanged. Optical radiation with frequency ω_1 passes through a nonlinear medium, and its spatial spectrum is recorded in focal plane 6. When the nonlinear medium is stimulated by external pumping on frequency ω_2 , additional components on frequency ω_1 can be observed at the output from the nonlinear medium. Special steps were taken to shape the spatial spectrum of the interacting waves in order to enable evaluation of changes in the spatial spectrum of the field re-radiated by the medium. Radiation with frequency ω_1 had a plane front, so that the width of its spatial spectrum corresponded to the diffraction limit. Radiation with frequency ω_2 had a pronounced spatial spectrum. A transparency mounted in the focal plane of lens 2 was used for this purpose.

The typical appearance of spatial spectra of the initial emission ω_1 , pumping radiation ω_2 and the field of the emission ω_1 re-radiated by the nonlinear medium is shown in Fig. 2 [photos not reproduced]. From the results we conclude that in this experiment we have observed a previously unstudied effect of transformation of the spatial spectrum of optical radiation upon passage through a nonlinear medium. This effect shows up as re-radiation of the energy of the plane wave by the stimulated nonlinear medium into spatial side frequencies whose spectrum corresponds to the autocorrelation function of the spatial pumping spectrum.

We have suggested two models to explain the change in the spatial spectrum of the field re-radiated by the excited nonlinear medium on the frequency of the investigated radiation: four-photon interaction $\omega_1 + \omega_2 - \omega_2 + \omega_1$ and two-stage interaction $\omega_1 + \omega_2 + \omega_{int}$; $\omega_{int} - \omega_2 + \omega_1$. Actually, if radiation ω_1 is a plane wave $E_{10} \exp [j(\omega_1 t - k_1 r)]$, and the pumping radiation is a spatially modulated wave $E_{20} \exp [j(\omega_2 t - k_2 r)]$, then in the given-field approximation, the amplitude of the field re-radiated by the medium as a result of the first interaction will be determined by the expression $\sigma_3 E_{10} |E_2(r)|^2 \exp j(\omega_1 t - k_1 z)$, and as a result of the second interaction--by the expression $\sigma_2^2 E_{10} |E_2(r)|^2 \exp j(\omega_1 t - k_1 z)$, where σ_2 , σ_3 are coefficients that characterize the efficiency of conversion on quadratic and cubic nonlinearities of the medium respectively.

These expressions imply that in both cases the fields re-radiated by the nonlinear medium have the same form, and differ only in intensity; the spatial spectrum of the field re-radiated by the medium is the autocorrelation of the spectrum produced by amplitude modulation of the pumping field; phase modulation of the pumping field should have no effect on the spatial spectrum of the field that is re-radiated by the medium on the frequency of the investigated emission.

Thus, both our models lead to the observed effect, and predominance of a given nonlinear process is determined by the ratio between effective values of quadratic and cubic nonlinearities of the medium, the power of the pumping radiation and so forth. In the experiment done by the authors, two-stage conversion predominated; moreover, this arrangement enabled us to overcome the considerable technical difficulties associated with the necessity of separating the radiation on frequency ω_1 transmitted through the medium from the emission on the same frequency re-radiated by the medium as a result of the nonlinear process. In this case it is possible to replace the simultaneous two-stage conversion with sequential conversion by separating the nonlinear medium into two different parts by a filter that transmits emission ω_2 and ω_{int} , but does not pass radiation ω_1 (see Fig. 3). The field of ω_1 at the output from the nonlinear medium in this arrangement contains only the component re-radiated by the medium as a result of the nonlinear

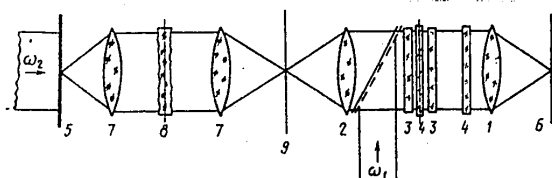


Fig. 3. Diagram of setup for observing spatially modulated radiation propagating through a phase-distorting medium

process. While the amplitude of this component has fallen to half, the simultaneously achieved suppression of the initial radiation by a factor of 10^6 yields the necessary positive effect. Since then, several authors have managed to observe analogous effects determined by four-frequency processes as well [Ref. 4, 5].

The given effect opens up new and interesting possibilities in the investigation of parameters of laser emission. The spatial spectrum of radiation is formed due to modulation of both amplitude and phase (see for example Ref. 6). In the experiment considered above, the spatial spectrum of the field re-radiated by the medium is dependent only on amplitude modulation of the radiation that excites this medium.

This property can be put to practical use for example where it is necessary to observe spatially modulated radiation propagating through a phase-distorting medium. A diagram of the corresponding experimental setup is shown in Fig. 3 (all notation is the same as in Fig. 1). Radiation ω_1 , as in the previously described experiment, is a plane wave. Radiation ω_2 is amplitude-modulated by a transparency mounted in the focal plane of lens 7, and phase-modulated by phase-distorting plate 8 mounted in the plane of the intermediate pupil of lenses 7. In plane 9 we register the spatial spectrum of radiation ω_2 modulated either with respect to amplitude only (when phase-distorting plate 8 is absent) (see Fig. 2b [photo not reproduced]), or with respect to both amplitude and phase (Fig. 4a [photo not reproduced]).

The spatial spectrum of radiation ω_1 at the output from the nonlinear medium is registered in plane 6, and is independent of whether the phase-distorting plate is present or absent (Fig. 2c and 4b [photos not reproduced]). The results confirm the previously drawn conclusions about the possibility of using the investigated effect to eliminate the influence of phase distortions of a medium when observing amplitude-modulated radiation through this medium.

A distinguishing feature of the investigated setup as compared with those based on the wavefront reversal effect [Ref. 7] is single rather than double passage of the radiation through the distorting medium, which is much more convenient for developing specific devices.

It should be noted that although the above discussion was addressed primarily to spatially modulated fields, in accordance with the space-time analogies that occur in the theory of nonlinear interactions of modulated waves (see for example Ref. 8) it can be assumed that the given effect is suitable for separating components of laser radiation associated with amplitude and phase modulations in time as well. Use of a method of this kind for studying the frequency spectra

FOR OFFICIAL USE ONLY

of optical radiation can be expected to be most effective in the investigation of ultrashort pulses.

REFERENCES

1. Matveyev, I. N., Kudryashov, V. A., Yermeyeva, R. A., "Tezisy dokladov sed'moy Vsesoyuznoy konferentsii po kogerentnoy i nelineynoy optike" [Abstracts of Papers at Seventh All-Union Conference on Coherent and Nonlinear Optics], Moscow, published by Moscow State University, 1974, p 477.
3. Ustinov, N. D., Matveyev, I. N., KVANTOVAYA ELEKTRONIKA, Vol 4, 1977, p 2995.
4. Blom, D. M., Bjorklund, G. C., APPL. PHYS. LETTS, Vol 31, 1977, p 592.
5. Voronin, E. S., Ivakhnik, V. V., Petnikova, V. M., Solomatin, V. S., Shuvalov, V. V., KVANTOVAYA ELEKTRONIKA, Vol 6, 1977, p 2009.
6. Rytov, S. M., "Vvedeniye v statisticheskuyu radiofiziku" [Introduction to Statistical Radio Physics], Moscow, Nauka, 1976, part 1.
7. Zel'dovich, B. Ya., Nosach, O. Yu., Popovich, V. I., Ragul'skiy, V. V., Fayzulov, F. S., VESTNIK MOSKOVSKOGO GOSUDARSTVENNOGO UNIVERSITETA, SERIYA III: FIZIKA, ASTRONOMIYA, Vol 19, No 4, 1978, p 137.
8. Akhmanov, S. A., Chirkin, A. G., "Statisticheskiye yavleniya v nelineynoy optike" [Statistical Phenomena in Nonlinear Optics], Moscow, published by Moscow State University, 1971.

COPYRIGHT: Izdatel'stvo "Radio i svyaz'", "Kvantovaya elektronika", 1981

6610

CSO: 1862/91

END